How Much of Gravitationally Induced Entanglement Is in the Eye of the Frame

Brecht Corbeel
Absolute Digital Publishers
absolutedigitalpublishers.com

September 19, 2026

Abstract. In the two-mass gravitationally induced entanglement protocol of Bose et al. and Marletto and Vedral, each mass sits in a two-branch superposition and the four branch pairs acquire Newtonian phases $\varphi_{ij} = Gm_A m_B t/(\hbar d_{ij})$. Local unitaries remove every pattern of the form $a_i + b_j$ exactly, leaving a single invariant, $\varphi_{\text{ent}} = \varphi_{LL} + \varphi_{RR} - \varphi_{LR} - \varphi_{RL}$, on which the state's negativity, $\mathcal{N} = |\sin(\varphi_{\text{ent}}/2)|/2$, and every standard witness depend and nothing else does. We analyse this state inside the quantum-reference-frame formalism of Giacomini, Castro-Ruiz and Brukner, restricted honestly to the translation group with ideal frames, and compute all three bipartite negativities in all three frames — the laboratory, the frame of mass A, and the frame of mass B. The entanglement structure is frame-covariant: what the laboratory describes as entanglement between the masses appears in A's frame partly as entanglement between B and the laboratory body, so "the masses became entangled" is not a frame-independent fact. The measured witness W, in either its fringe-correlation or spin-witness form, is a function of φ_{ent} and locally removable phases only; since every branch-pair distance is relational, φ_{ent} is invariant under the model's frame group and W is a scalar. Every frame therefore agrees on the experiment's outcome while disagreeing on which subsystems carry the entanglement that explains it. We restate what a positive result certifies in invariant form — no local-operations-and-classical-communication channel between the branch sectors reproduces the correlations, in any frame — and sort the published objections by whether they attack this invariant content or only the covariant sentence about A and B; at least one prominent dispute dissolves under the split, and the strongest counter-case is given its full force. With branch dephasing at rate γ the interference terms carry the exact factor $e^{-\gamma t}$ while φ_{ent} is unchanged, which yields the detection threshold $\varphi_{\text{ent}}^{\min}(\gamma t, \text{shots})$ that experiment designers need. Every extension beyond the toy model's translation group is flagged as speculative; a seeded simulation reproduces every table entry and curve.

Keywords: gravitationally induced entanglement; BMV protocol; quantum reference frames; negativity; entanglement witness; frame covariance; Newtonian gravity; branch dephasing.
Series: The Quantum–Relativity Papers, No. 3.

1 Introduction

Two masses, each split into a two-branch spatial superposition and held apart for a time t, acquire a different relative phase for each pairing of branches, and the four phases do not in general factorize. That is the entire mechanism of the gravitationally-induced-entanglement proposal of Bose, Mazumdar, Morley, Ulbricht and collaborators [13], whose companion inference — that any system able to mediate entanglement between two quantum systems must itself be non-classical — is Marletto and Vedral's [47] and is advanced there as *sufficient*, not necessary, evidence of quantum effects in gravity. In the Newtonian regime the two-mass state is

$$|\Psi\rangle \;=\; \tfrac{1}{2}\sum_{ij} e^{i\varphi_{ij}}\,|i\rangle_A|j\rangle_B, \qquad \varphi_{ij} \;=\; \frac{G\,m_A m_B\,t}{\hbar\,d_{ij}}, \quad (1)$$

with d_{ij} the separation between branch i of mass A and branch j of mass B, and $i,j \in \{L,R\}$. Local unitaries on either mass remove exactly the part of the pattern that factorizes as $\varphi_{ij} = a_i + b_j$, leaving one surviving combination, $\varphi_{\text{ent}} = \phi_{LL} + \phi_{RR} - \phi_{LR} - \phi_{RL}$, and the negativity of the state is $\mathcal{N} = |\sin(\varphi_{\text{ent}}/2)|/2$ (Proposition 1, §2, derived in Appendix A). Every standard BMV witness is a function of φ_{ent} and of nothing else the experiment can vary.

What a measured $\varphi_{\text{ent}} \neq 0$ certifies has been argued over since the proposals appeared. Hall and Reginatto showed the step from observed entanglement to a quantum mediator carries a further assumption — that a classical interaction cannot entangle — and constructed a configuration-ensemble model in which it does [39]. Anastopoulos and Hu, in an arXiv comment that was never accepted as a published Comment and which we cite as the preprint it is, hold that Newtonian gravity-induced entanglement is "agnostic to the quantum or classical nature of the gravitational true degrees of freedom" [5]. Fragkos, Kopp and Pikovski argue that relativity does not fix the mediator-versus-nonlocal-process distinction the inference rests on [30], and Martín-Martínez and Perche reach the setup through quantum field theory and conclude that a linearized, weak-field treatment already suffices to produce the entanglement [50]. Against that: Galley, Giacomini and Selby's theory-independent trilemma, in which "gravity can entangle," "gravity mediates" and "gravity is classical" cannot all hold [33]; Christodoulou and Rovelli's reading of the effect as a superposition of proper times and hence of geometries [20]; Belenchia, Wald, Giacomini, Castro-Ruiz, Brukner and Aspelmeyer's causality argument that the field of a superposed source must carry quantum information [11]. The dispute has not closed: Trillo and Navascués show the Diósi–Penrose classical model predicts the entanglement [67], Struyve proves a different semiclassical family does not [64], and Di Biagio locates the tension in an information-theoretic rather than spatiotemporal notion of locality smuggled into the no-go theorems [28].

We add a prior question that literature does not ask — the frame relative to which "A and B became entangled" is supposed to be a fact. Giacomini, Castro-Ruiz and Brukner's quantum-reference-frame transformations already answer that entanglement, and superposition itself, are not frame-independent properties [36]; Vanrietvelde, Höhn, Giacomini and Castro-Ruiz recast frame choice as gauge-fixing inside a perspective-neutral space [69]; de la Hamette and Galley extend the construction to general symmetry groups [25]; and Krumm, Höhn and Müller supply the relational trace without which a third, spectator body is mishandled after a frame jump [45] — the exact hazard in a three-body lab. That entanglement is frame-relative is old news in relativistic quantum information: Peres and Terno [56], Peres, Scudo and Terno [55] and Gingrich and Adami [38] established it for boosts, and Zanardi [72], Zanardi, Lidar and Lloyd [73] and Harshman and Ranade [40] established the more general point that which subsystems exist is fixed by the accessible observables. The novelty here is not that entanglement moves. It is that the thing the experiment actually measures does not.

Our claims are exactly these, graded where each synthetic step is taken:

(a) the explicit three-frame computation of the BMV state and of every bipartite negativity in the laboratory frame, in mass A's frame and in mass B's frame, exhibiting concretely how lab-frame A:B entanglement reappears partly as B:C entanglement once A is the frame — ours as computation, exact within the translation-group model (Proposition 2, §4, Figure 1, Appendix A);

(b) the theorem that the branch-pair distances d_{ij} are relational, so $\varphi_{\rm ent}$ and the measured witness W are invariant under the model's frame group and under local unitaries alike — exact, and the reason all three frames agree on the outcome while disagreeing about which parties carry the entanglement that explains it (Proposition 3, §4, Appendix A);

(c) the operational restatement of what a positive result certifies, splitting the invariant content (no local-operations-and-classical-communication channel between branch sectors reproduces the correlations, in any frame) from the frame-dependent content ("gravity entangled A with B"), and sorting the published objections by which half they attack — structured and argued, not derived, with Anastopoulos and Hu's case given its full force (Proposition 4, §5);

(d) the robustness bound: branch dephasing at rate γ leaves $\varphi_{\rm ent}$ untouched and multiplies the interference terms by $e^{-\gamma t}$, yielding a detection threshold $\varphi_{\rm ent}^{\rm min}(\gamma t, \text{shots})$ — exact within the dephasing model (Proposition 5, §6, Figure 2, Appendix B).

The threshold in (d) is the quantity a designer bargains over, and the bargaining is already tight. Schut and Mazumdar's parameter scan puts the test-mass scale at 10^{-14} kg and the unscreened design at roughly 450 μm separation with a 200 μm superposition, falling to about 35 μm separation and at least 1 μm superposition once electromagnetic screening is introduced, against a tolerable decoherence rate near 10^{-3} Hz [62]; Tilly, Marshman, Mazumdar and Bose find that rejecting the no-entanglement hypothesis at 99.9% confidence costs $O(10^3)$ measurements at negligible decoherence and $O(10^6)$ past a rate of 0.125 Hz [66]. For scale, the smallest masses whose Newtonian coupling has been measured at all are the 90 mg gold spheres of Westphal, Hepach, Pfaff and Aspelmeyer, resolved across a 400 μm minimal surface separation over 350 hours of integration [71]. A frame-invariant target is worth naming before that budget is spent.

§2 derives Proposition 1 and situates it in the proposal literature and its actual parameter ranges. §3 states the frame formalism honestly — translation group, ideal frames, and what is thereby idealized away, including the frame-change decoherence Palmer, Girelli and Bartlett prove unavoidable for real frames [53] and the record-keeping conditions under which a frame counts as classical at all [22]. §4 carries the three-frame computation and the invariance proof. §5 does the sorting, and names the one published dispute that dissolves under the split rather than being settled by it. §6 derives the dephasing bound — the same visibility bookkeeping that governs interferometric coherence generally [21] — states what measurement would falsify the picture, and hands the optimization problem forward. Appendix A holds the negativity algebra and the three-frame table, Appendix B both witness forms and the dephasing derivation, and Appendix C the computation behind the figures.

2 The protocol's entire signal is a single phase combination

The two-mass protocol analysed in this paper is not ours. Bose, Mazumdar, Morley, Ulbricht, Toroš, Paternostro, Geraci, Barker, Kim and Milburn proposed placing two mesoscopic masses, each carried through a two-branch matter-wave interferometer, close enough that gravity is their only coupling, and reading the resulting spin–spin entanglement as a witness that the mediating field carried coherent off-diagonal terms [13]. Marletto and Vedral supplied the companion information-theoretic argument in the same journal issue: a system that can mediate entanglement between two quantum systems must itself be non-classical, so gravitationally induced entanglement is *sufficient* evidence of quantum effects in gravity without any direct quantum control of the field — and their own framing is careful that this is sufficiency, not necessity [47]. Marshman, Mazumdar and Bose later grounded the inference in relativistic field theory and in local-operations-and-classical-communication bookkeeping, identifying micro-causality rather than any particular graviton picture as the load-bearing assumption [49]. The programme's current synthesis across platforms and mass scales is the 2025 review by Bose and collaborators [14], and its present institutional shape is a spin-based nanodiamond roadmap whose authors state plainly that realization needs a medium-sized consortium with excellent suppression of vibrational and gravitational noise [15]. Nothing in this section is offered as new physics; the section exists to fix, exactly, what quantity the experiment actually measures, because Sections 3 and 4 will show that this quantity and the entanglement it is usually described as measuring behave differently under a change of quantum reference frame.

The model is the standard one. Two masses m_A and m_B, each held in a superposition of two spatial branches labelled L and R, are allowed to interact for a time t through the Newtonian potential alone; each of the four branch pairs (i, j) sits at its own centre-to-centre separation d_{ij}, held fixed during the interaction, and accumulates its own dynamical phase. The idealization is severe and deliberate: no retardation, no internal structure, no motion of the branches during the hold, and exactly two branches per mass.

Proposition 1 (The BMV state and its invariant phase)**.** *Two masses, each in a two-branch superposition, interacting gravitationally for time t in the Newtonian regime:*

$$|\Psi\rangle = \tfrac{1}{2}\sum_{ij} e^{i\varphi_{ij}}|i\rangle_A|j\rangle_B, \qquad \varphi_{ij} = \frac{G\,m_A m_B\,t}{\hbar\,d_{ij}}. \tag{2}$$

Local unitaries remove the pattern $\varphi_{ij} = a_i + b_j$ exactly; the residual

$$\varphi_{\text{ent}} = \phi_{LL} + \phi_{RR} - \phi_{LR} - \phi_{RL} \tag{3}$$

is the sole local-unitary invariant; entanglement (negativity $\mathcal{N} = |\sin(\varphi_{\text{ent}}/2)|/2$ for this state, derived in Appendix A) and every standard BMV witness are functions of φ_{ent} alone.

The counting behind the second clause is exact and worth stating, because the rest of the paper leans on it. The four phases $\phi_{LL}, \phi_{LR}, \phi_{RL}, \phi_{RR}$ carry four real parameters. A local phase gate on each mass, $\mathrm{diag}(e^{ia_L}, e^{ia_R}) \otimes \mathrm{diag}(e^{ib_L}, e^{ib_R})$, shifts them by the additive pattern $a_i + b_j$, which has four parameters of which one is a global phase already unobservable — three independent directions in the four-dimensional phase space. Exactly one direction survives, and φ_{ent} spans it. This is not a weak-coupling expansion or a small-entanglement limit: within the two-branch truncation it holds for every geometry, every mass, and every interaction time. Everything an experimenter can do locally — shifting an interferometer's recombination phase, redefining which branch is called L, letting the two arms accumulate unequal non-gravitational phases — moves the state along the three removable directions and leaves φ_{ent} where it was.

The geometry enters only through the four separations, and for the arrangement the proposals actually draw — two parallel interferometers with both splittings Δx along the line joining them, the near branches separated by d — the assignment is $d_{LL} = d_{RR} = d$, $d_{LR} = d + \Delta x$, $d_{RL} = d - \Delta x$, so that

$$\varphi_{\text{ent}} = \frac{Gm_A m_B t}{\hbar}\left(\frac{2}{d} - \frac{1}{d+\Delta x} - \frac{1}{d-\Delta x}\right) = -\frac{2\,Gm_A m_B t\,\Delta x^2}{\hbar\,d^3}\cdot\frac{1}{} \tag{4}$$

where the second equality is exact algebra, not an expansion. The familiar quadrupole-scaling statement that the entangling phase goes as $\Delta x^2/d^3$ is the first factor alone, and it is a poor approximation precisely where the proposals want to operate: at the parameter-scan point $d \simeq 450\,\mu$m with $\Delta x \simeq 200\,\mu$m reported by Schut and Mazumdar [62], $\Delta x/d$ is $4/9$ and the exact bracket is larger than the quadrupole term by the factor $1/[1 - (\Delta x/d)^2] = 81/65 \simeq 1.25$, so the leading term recovers only about 80% of the phase. This is our arithmetic on their geometry, exact given Eq. (2), and it cuts in the experiment's favour rather than against it.

The parameter ranges the proposals commit to are narrower than the field's rhetoric suggests, and they are worth writing down at the numbers. The QGEM parameter scan of Schut and Mazumdar [62] works at a test-mass scale of 10^{-14} kg and reports that the original, unscreened design needs a separation of about $450\,\mu$m with a superposition size of about $200\,\mu$m, that electromagnetic screening cuts the separation requirement to about $35\,\mu$m with a minimum superposition size of

$1\,\mu$m, and that the tolerable decoherence rate is about 10^{-3} Hz. The Casimir-screening design of van de Kamp et al. [68] pushes the mass down to 10^{-16}–10^{-15} kg at $\Delta x \sim 20\,\mu$m, at the cost of a 10^4 T/m field gradient and a conducting plate between the arms whose own vibrational modes become a decoherence channel. Put those into Eq. (4) with $G = 6.674 \times 10^{-11}\,\mathrm{m^3kg^{-1}s^{-2}}$ and $\hbar = 1.0546 \times 10^{-34}$ J s: the unscreened point accumulates $|\varphi_{\rm ent}|$ at $6.9 \times 10^{-2}\,\mathrm{rad\,s^{-1}}$, reaching one radian in 14 s and π in 45 s, while the screened point accumulates it at $3.0 \times 10^{-3}\,\mathrm{rad\,s^{-1}}$, needing 340 s and 1.1×10^3 s for the same two marks. These four numbers are ours, exact arithmetic on the two cited geometries and nothing else.

That factor of 23 between the two phase rates is the screening trade stated honestly, and it is a design fact the scan's headline numbers hide. Shrinking d by a factor of 13 helps as d^{-3}; shrinking Δx from $200\,\mu$m to $1\,\mu$m hurts as Δx^2, and the second effect wins by more than an order of magnitude. Screening buys a superposition size that levitated platforms might plausibly reach — the delocalization records are still far short, with a threefold expansion beyond zero-point motion demonstrated for a levitated nanosphere [59] and optimal-control protocols proposed to go substantially further [70] — and it pays for that with an interaction time an order of magnitude longer, during which the same decoherence rate does correspondingly more damage. Combining the scan's own 10^{-3} Hz with its own screened geometry through the dephasing algebra of Appendix B gives a maximum achievable witness value of 0.86, below the separability bound of unity, whereas the unscreened geometry at the same rate reaches 1.91 at $t \simeq 45$ s; we grade this comparison structured rather than exact, because it pairs rows of a single parameter scan that may not describe one self-consistent operating point, and because our single-rate branch-dephasing model is not necessarily the decoherence model the scan used. Read at that grade it is still a live warning: the screened design's margin against decoherence is thinner than its smaller apparatus suggests.

Against those targets, what laboratories have actually done with gravity and with mass superpositions separately is instructive and not encouraging about the gap. Westphal et al. [71] measured Newtonian coupling between two gold spheres of 90 mg at a minimal surface separation of $400\,\mu$m, with 350 hours of integration and a systematic accuracy of $4\times10^{-11}\,\mathrm{m/s^2}$ — classical gravity, at a mass twelve orders above the QGEM scale. Fuchs et al. [31] sense kilogram source masses with a 0.4 mg superconducting particle at a force noise of $0.5\,\mathrm{fN}/\sqrt{\mathrm{Hz}}$; Miki et al. [51] argue that entanglement between 7 mg mirrors is achievable in the short term, but by continuous measurement and feedback-generated squeezing rather than by the bare gravitational phase of Eq. (2). On the superposition side, the all-magnetic chip interferometer of Pino et al. [57] targets a sphere of $\gtrsim 10^{13}$ atomic mass units delocalized over about half a micrometre, which is the right mass scale and roughly the screened design's Δx — as a design target, not a result. No apparatus has yet held a QGEM-scale mass in a QGEM-scale superposition, and the protocol's whole difficulty is that both halves are needed at once.

Two witness forms appear in the literature and Appendix B treats both. The fringe-correlation form recombines each interferometer with an adjustable phase offset and correlates the two output ports; the spin-witness form reads a spin degree of freedom whose projection along the Stern–Gerlach axis records which branch the mass took. They are usually presented as two readouts of the same thing, and Proposition 1 guarantees both are functions of $\varphi_{\rm ent}$ and of locally removable phases alone. They are not, however, equally informative: we show in Appendix B that the correlator built purely from recombination-plane settings factorizes exactly, as a product of one function of each interferometer's own offset, so no witness assembled from fringe correlations alone can exceed the separability bound at any $\varphi_{\rm ent}$. Fringe correlations measure the phase; they certify entanglement only through the two-branch model that converts a phase into a negativity. A model-independent entanglement witness needs at least one which-branch reading. That is an exact statement about the state of Eq. (2), it explains why the original proposal's witness mixes a recombined setting on one mass with a which-branch setting on the other, and it is the first of several places in this paper where two quantities that the literature treats as interchangeable come apart under examination.

The boundaries of this section's model should be named before Section 3 builds on it. The Newtonian phase of Eq. (2) discards retardation, and Christodoulou et al. [19] argue from linearized quantum gravity that retarded entanglement generation, not the instantaneous Newtonian phase, is the signature that cannot be reproduced by an instantaneous interaction — a sharper target than the one this protocol aims at, though they propose it as more tractable in the electromagnetic analogue than in the gravitational case. The two-branch truncation discards the spatial modes a real interferometer carries, and Chevalier et al. [18] identify an experimental loophole in exactly that gap, closable by state tomography, alongside a statistical method for separating the gravitational contribution from unknown background interactions. The single-rate dephasing model of Appendix B is not the only decoherence channel in play: Rijavec et al. [58] find that under Continuous Spontaneous Localization any value of the collapse model's parameters would completely hinder the generation of gravitationally induced entanglement, which is a categorical claim about a modification of quantum mechanics rather than about environmental noise, and which our γ does not represent. And the whole protocol is one of several routes: Krisnanda et al. [44] show that released masses in free fall can accumulate detectable entanglement faster than their coherence times without any macroscopic superposition developing, while Pedernales et al. [54] amplify the coupling with a massive intermediary whose effective strength grows with its mass and is independent of its temperature. Section 5 returns to what all of these would and would not establish; the present section has fixed only what they measure.

3 Jumping to the frame of a superposed mass relabels relative data and nothing else

The computation in Section 4 rewrites the two-mass state of Section 2 from the perspective of one of the interfering masses, and every claim the paper makes afterwards depends on that rewriting being a theorem rather than a figure of speech. We therefore fix the formalism here, at the narrowest scope in which the question can still be posed, and we state the cost of the narrowness before spending it: what follows is a translation-group quantum reference frame (QRF) construction, three bodies, ideal frames, and the Newtonian interaction entering as an external c-number potential on the relative configuration. That is strictly less than a theory of superposed geometries and is not offered as one. The narrowness is not modesty for its own sake. It is the reason the invariance statement of Section 4 is provable rather than plausible: in this model the group under which the witness is asserted to be invariant is written down explicitly, and its action on every quantity in the problem can be checked by hand, which is what Appendix A does.

3.1 The frame is a body in the Hilbert space, and that exhausts the idea

Nothing in the QRF programme requires an observer, a perspective in any phenomenological sense, or a change in the physical situation. A frame is a physical system, and a description "relative to" it is a description written in coordinates referred to that system. The lineage predates the formalism by half a century: Aharonov and Susskind [2] showed that a relative phase forbidden by a superselection rule becomes observable once a suitable reference system is admitted into the description, Aharonov and Kaufherr [1] treated the frame itself as a quantum system carrying its own position and orientation uncertainty, and Bartlett et al. [9] made the idea a resource theory in which frame information is unspeakable, quantifiable and depletable. What Giacomini et al. [36] added, and what makes the present computation possible at all, is an explicit unitary carrying the description relative to one body into the description relative to another — including when the second body is in a superposition of positions relative to the first.

We use that transformation in one spatial dimension for three bodies: the two masses A and B, and a laboratory body C. Relative to C the state lives on $\mathcal{H}_A \otimes \mathcal{H}_B$ in the relative coordinates x_A and x_B, and C carries no state of its own, because its position relative to itself is zero by construction. The change to A's perspective is

$$\hat{S}_{C\to A} = \hat{\mathcal{P}}_A \exp\Big[\tfrac{i}{\hbar}\,\hat{x}_A\hat{p}_B\Big], \tag{5}$$

a parity operation on the old frame body composed with a translation of B controlled by A's position, acting on the position basis as $|x_A\rangle_A|x_B\rangle_B \mapsto |-x_A\rangle_C|x_B - x_A\rangle_B$ [36]. The bookkeeping is the content: after the map A has become the frame and has no state, while C has become a system whose position is referred to A. Reading Eq. (5) as a relabelling rather than a physical operation is exact within the model, not an interpretive gloss — the map is invertible, carries observables along with states, and consumes no time.

3.2 Gauge fixing is what the jump is, and that settles what the jump cannot do

The reading we adopt is the perspective-neutral one. Vanrietvelde et al. [69] construct a gauge-invariant Hilbert space in which adopting a particular frame's perspective is a gauge fixing and switching frames is a gauge transformation, and show in a one-dimensional model of interacting particles that entanglement and classicality of an observed subsystem are perspective dependent in exactly this sense. Höhn et al. [41] prove that the Dirac-quantized, Page–Wootters, and relational-Heisenberg descriptions of such a system are the same theory viewed through different reduction maps, and de la Hamette et al. [26] extend the construction to general unimodular Lie groups. We take from this literature one structural commitment and one prohibition. The commitment: there is a single frame-independent object, and the perspectives are its gauge fixings. The prohibition: nothing physical happens during a frame change, so no statement of the form "the entanglement was created by the jump" is available to us, and equally none of the form "the jump destroyed it."

That prohibition also sets what the invariance result of Section 4 is allowed to mean. Because $\hat{S}_{C\to A}$ transports states and measurement operators together, the predicted statistics of any fixed physical measurement are frame independent by construction, and a theorem asserting only that would be empty. The non-trivial claim is narrower and is about a particular number: the four-configuration phase combination φ_{ent} is built from relational distances that the group action leaves pointwise fixed, which is a property of the interaction and the geometry rather than a tautology about covariance.

Three bodies is also where the formalism first bites. Krumm et al. [45] show that after a jump to a second particle's perspective the naive partial trace misassigns what belongs to a third, bystander system, and introduce a relational trace to repair it. Their theorem is proved for finite Abelian groups and our translation group is Abelian but not finite, so we treat their result as a constraint we respect rather than a theorem we invoke, which is a structured rather than exact use of their work: in Appendix A every reduced state is taken inside the reduced Hilbert space that the frame's own gauge fixing supplies, and we never trace over the body that is serving as the frame. A second caution comes from Höhn and Vanrietvelde [42], who find genuine discontinuities in relational dynamics across a switch between quantum clocks; our frames are spatial and the switch is made at a fixed instant of the laboratory parameterization, so that discontinuity is not inherited, but it is a live hazard for any extension of this paper to temporal frames.

3.3 The scope is narrow on purpose, and each exclusion is load-bearing

Three exclusions matter, and we would rather name them than have them found. First, the group. We use spatial translations only. de la Hamette and Galley [25] give the QRF construction for general symmetry groups including non-Abelian ones, Giacomini et al. [37] and Apadula et al. [7] extend it to superpositions of Lorentz boosts, and Ballesteros et al. [8] show that the momentum-dependent QRF transformations of the original construction close into a Lie algebra distinct from the classical Galilei algebra. Any claim that our results survive into those larger groups is speculative, and we mark it as such wherever we make one.

Second, the frames are ideal. Palmer et al. [53] prove that changing between genuine quantum reference frames necessarily induces decoherence on the systems described relative to them, and Bartlett et al. [10] show that a finite directional frame built from N spins supports only order N^2 high-precision measurements before it degrades. Our frame bodies neither decohere nor wear out. That idealization is harmless for the invariance theorem, which concerns a phase built from relational distances, and is not harmless for any claim about what an experimenter located on mass A could actually do — a distinction we keep explicit in Section 5.

Third, the interaction. Gravity enters as a c-number potential evaluated on branch-pair separations, which is the regime the proposals themselves analyze, and not as a field with its own state and its own transformation law. Christodoulou and Rovelli [20] read the same effect covariantly as a superposition of proper times, Belenchia et al. [11] and Belenchia et al. [12] argue from causality that the field sourced by a superposed mass must itself carry quantum information, and Martín-Martínez and Perche [50] redo the setup in quantum field theory. Meanwhile the QRF programme has been pushed well past our toy model: to superpositions of proper time and gravitational redshift [34], to the equivalence principle for superposed fields [17, 35], to the temporal localizability of events sourced by gravitating superpositions [16], and to field states on superposed geometries [43]. We inherit none of that machinery and claim none of its reach.

3.4 Operationally the jump is a dictionary between two records, not a trip

The operational content of "the frame of mass A" is a translation manual. Two experimenters hold the same list of laboratory events; one writes every position as a displacement from C, the other as a displacement from A; Eq. (5) is the rule converting the first list into the second, and the conversion is exact and information preserving. Nobody rides the mass. The reason the manual is interesting rather than trivial is that it does not act on the two registers separately: the translation of B is controlled by A's position operator, so a state that factorizes in one list need not factorize in the other, and the tensor product structure itself is what changes. That this is a physically forced instance of a much more general fact, rather than a QRF curiosity, is a structured reading we endorse: Zanardi [72] and Zanardi et al. [73] show that the partition of a system into subsystems is induced by the accessible observable algebra, and Harshman and Ranade [40] construct, for any fixed pure state, observables giving it any entanglement value one likes. The QRF jump is the case in which the repartition is not a free choice of the theorist but a consequence of which body carries the rulers.

Frame relativity of entanglement-adjacent quantities is likewise not news, though the existing results are of a different kind and conflating them with ours would be an error. Boosts spoil the covariance of the reduced spin state and of spin entropy [23, 55, 56], trade spin entanglement against momentum entanglement while preserving the total [38], and force EPR measurement directions to be reboosted before anticorrelation returns [65]; acceleration degrades entanglement outright through the Unruh effect [3, 4, 32], and a fully quantum noninertial frame reaches the same verdict that no description of a state is absolute [6]. Ours is a translation-group result in a Galilean setting, and its mechanism — a position-controlled repartition rather than a Bogoliubov mixing of modes — is not theirs, so the analogy is structured and we import none of their formulas.

The relational stance underneath all of this is Rovelli [60]'s: states are relations between systems rather than observer-independent facts, a reading also at work in the relational treatment of clocks [63] and, in a more radical form we do not need, in the process-matrix framework where causal order itself is indefinite [52]. One neighbouring claim needs separating from ours. Foo et al. [29] argue that when superposed amplitudes differ only by a coordinate transformation, the scenario can be rewritten on a single fixed background, so the associated decoherence is an artifact of the external systems fixing the relative coordinates. Their "frame" is a coordinate chart; ours is a physical body with a Hilbert space, and a jump between bodies is not a relabelling of a chart. Treating their conclusion as support for ours would be a structured borrowing at best, and we do not rest anything on it. The orientation-dependent version of the same relational bookkeeping is developed in Corbeel [22], and the interferometric consequences of frame-relative phase in Corbeel [21].

4 Jumping into a superposed mass moves the entanglement without moving the measurement

Section 2 described the interferometer pair relative to the laboratory, and Section 3 named what that description suppresses: the laboratory is a third body, C, whose translational degree of freedom has been silently promoted to a coordinate system. Restoring it is a precondition for the question this section asks rather than a refinement of the model, because a quantum reference frame transformation maps between descriptions relative to different physical bodies [36], and a description has to have a body to transform to. We therefore carry three systems — A, B, C — and one convention, stated here because every zero in Table 1 depends on it: in the perspective of a given body, that body carries the trivial one-dimensional factor, so a bipartition containing the frame itself has negativity zero by construction and not by computation. Fixing a perspective is a gauge fixing rather than a physical operation [69], and those zeros record the gauge, not an absence of correlation in the world. We write $\mathcal{N}_{AB}$, $\mathcal{N}_{AC}$, $\mathcal{N}_{BC}$ for the negativities across the three cuts.

Proposition 2 (Frame-covariance of the entanglement structure; exact, ours as computation)**.** *In the translation-group QRF model (masses A, B plus laboratory frame body C, relational coordinates), transforming to the frame of A maps the state to one in which A is definite and the branch structure — and with it the entanglement — lives on (B, C). All three bipartite negativities in all three frames are fixed by the algebra of Appendix A and collected in Table 1; the "A–B entanglement" of the lab frame appears partly as B–C entanglement in A's frame. Entanglement between the masses is not a QRF scalar.*

4.1 In mass A's own frame the interferometer is not superposed and the laboratory is

Let a_L, a_R locate A's two branches relative to C and b_L, b_R locate B's, with arm widths $\Delta_A = a_R - a_L$ and $\Delta_B = b_R - b_L$ and branch-pair distances $d_{ij} = |b_j - a_i|$. The lab-frame state of Section 2 is

$$|\Psi^{(C)}\rangle = \tfrac{1}{2}\sum_{i,j} e^{i\varphi_{ij}}\,|a_i\rangle_A|b_j\rangle_B, \qquad \varphi_{ij} = \frac{Gm_Am_Bt}{\hbar\, d_{ij}}. \tag{6}$$

The translation-group transformation into A's perspective acts on configuration basis states by $|a_i\rangle_A|b_j\rangle_B \mapsto |{-a_i}\rangle_C|b_j - a_i\rangle_B$ — exactly the non-relativistic case of Giacomini et al. [36], whose dependence on the reference particle's momentum closes into the enlarged algebra identified by Ballesteros et al. [8]. It is a relabelling of basis states, so the coefficients ride along untouched:

$$|\Psi^{(A)}\rangle = \tfrac{1}{\sqrt{2}}\sum_{i}|{-a_i}\rangle_C\otimes|\beta_i\rangle_B, \qquad |\beta_i\rangle = \tfrac{1}{\sqrt{2}}\sum_{j} e^{i\varphi_{ij}}|b_j - a_i\rangle. \tag{7}$$

Three readings of Eq. (7) are worth separating. A is now a definite body at its own origin. C — the granite table, the shielding, the readout rack — is in a two-branch superposition of $-a_L$ and $-a_R$, which is A's superposition wearing the opposite sign. And B occupies a superposition over the displaced positions $b_j - a_i$, which is where the gravitational phases have gone.

The whole computation then collapses to one overlap. Provided the branches are resolved — an idealization we return to below, exact within it — the two frame states $|{-a_L}\rangle_C$ and $|{-a_R}\rangle_C$ are orthogonal, so Eq. (7) is a two-term Schmidt decomposition whose reduced eigenvalues are $\lambda_\pm = \frac{1}{2}(1 \pm |\langle\beta_L|\beta_R\rangle|)$ and whose negativity is $\sqrt{\lambda_+\lambda_-}$ (exact, the standard pure-state expression). The lab frame obeys the same formula with $|\langle\beta_L|\beta_R\rangle|$ replaced by $|\cos(\varphi_{\rm ent}/2)|$, which is how $\mathcal{N}_{AB} = \frac{1}{2}|\sin(\varphi_{\rm ent}/2)|$ arises in Section 2. Everything that distinguishes the frames is therefore one inner product, and that inner product is fixed by geometry alone.

Two cases exhaust it, and they differ by whether two of the four displaced positions coincide. The coincidence $b_L - a_R = b_R - a_L$ would require $\Delta_B = -\Delta_A$ and never happens; the coincidence $b_L - a_L = b_R - a_R$ happens exactly when $\Delta_A = \Delta_B$. With generic arms, $\Delta_A \neq \Delta_B$, all four kets are distinct, $\langle\beta_L|\beta_R\rangle = 0$, and $\mathcal{N}_{BC} = 1/2$ — the maximum a two-term Schmidt state can carry. With symmetric arms, $\Delta_A = \Delta_B = \Delta$, one ket is shared, $\langle\beta_L|\beta_R\rangle = \frac{1}{2}e^{i(\phi_{RR}-\phi_{LL})}$, and $\mathcal{N}_{BC} = \sqrt{3}/4 \approx 0.433$. Neither value contains $\varphi_{\rm ent}$. Both survive the limit $G \to 0$ unchanged, which is the sharpest statement Proposition 2 admits: with gravity switched off entirely, the lab frame sees a product state and A's frame sees $\sqrt{3}/4$ of negativity across the only cut it has.

Symmetric arms are the experimentally interesting case, not the exceptional one, because a two-interferometer design uses the same superposition width on both sides; the screened QGEM parameter scan of Schut and Mazumdar [62] pairs 10^{-14} kg masses at a separation of $\approx 35\,\mu$m with a superposition size of at least $1\,\mu$m. In that collinear symmetric geometry $d_{LL} = d_{RR} = d$ exactly, so $\phi_{LL} = \phi_{RR}$, the overlap

Table 1: Bipartite negativities of one physical state, computed in three quantum reference frames, for symmetric arms $\Delta_A = \Delta_B = \Delta$; the algebra is in Appendix A. A bipartition containing the frame body carries the trivial factor and is zero by the convention of this section, not by computation. Generic arms, $\Delta_A \neq \Delta_B$, replace $\sqrt{3}/4$ by 1/2 throughout. The witness column is the same function of the same invariant in every row.

Frame	$\mathcal{N}_{AB}$	$\mathcal{N}_{AC}$	$\mathcal{N}_{BC}$	W
Gravity on, $\varphi_{\text{ent}} \neq 0$				
Lab body C	$\frac{1}{2}\lvert\sin(\varphi_{\text{ent}}/2)\rvert$	0	0	$W(\varphi_{\text{ent}})$
Mass A	0	0	$\sqrt{3}/4$	$W(\varphi_{\text{ent}})$
Mass B	0	$\sqrt{3}/4$	0	$W(\varphi_{\text{ent}})$
Gravity off, $\varphi_{\text{ent}} = 0$				
Lab body C	0	0	0	$W(0)$
Mass A	0	0	$\sqrt{3}/4$	$W(0)$
Mass B	0	$\sqrt{3}/4$	0	$W(0)$

above is real and positive, and the invariant closes in elementary form,

$$\varphi_{\text{ent}} = \frac{Gm_Am_Bt}{\hbar}\left(\frac{2}{d} - \frac{1}{d-\Delta} - \frac{1}{d+\Delta}\right) = -\frac{2\,Gm_Am_Bt\,\Delta^2}{\hbar\,d\,(d^2-\Delta^2)}, \tag{8}$$

exact for that geometry and the origin of the familiar Δ^2/d^3 scaling of the signal. Putting that scan's numbers into Eq. (8) with an illustrative one-second interaction — their geometry, our arithmetic, exact given those inputs — gives $|\varphi_{\text{ent}}| \approx 3 \times 10^{-3}$ radians and a lab-frame negativity $\mathcal{N}_{AB} \approx 7 \times 10^{-4}$, some six hundred times smaller than the $\sqrt{3}/4$ that the same physical state carries across the B–C cut in A's frame.

Table 1 collects the nine entries, and Fig. 1 draws the same apparatus three times with a negativity bar on each bipartition. The reshuffling is not the transfer of a conserved quantity, and saying so is the honest reading of the arithmetic: the B–C block in A's frame is dominated by kinematic correlation that is present with gravity off, so what the lab frame reports as the whole of the A–B negativity reappears only partly as B–C negativity and partly as a relative-phase pattern inside $|\beta_L\rangle$ and $|\beta_R\rangle$, which is local to B. Describing that as "the entanglement moved" is a structured step, not an exact one; what is exact is the pair of numbers and the fact that no frame's number is the privileged one.

4.2 Branch-pair distances are differences, so the measured phase never learns which body was called the origin

Proposition 3 (Invariance of the witness; exact)**.** *Branch-pair distances d_{ij} are relational quantities, so each φ_{ij} — and a fortiori φ_{ent} — is invariant under the model's QRF group; the measured witness W (fringe-correlation or spin-witness form, both treated in Appendix B) is a function of φ_{ent} and of locally removable phases only, hence W is a QRF scalar. Every frame agrees on the experiment's outcome while disagreeing on which subsystems carry the entanglement that explains it.*

The proof is three exact steps and no approximation. First, $d_{ij} = |b_j - a_i|$ is a difference of configuration coordinates, and the frame change $x \mapsto x - a_i$ preserves every difference, so each φ_{ij} is literally the same real number in all three descriptions; the displayed transformation above shows it, since the map permutes kets and leaves $e^{i\varphi_{ij}}$ attached to the branch pair that generated it. Second, the local-unitary freedom is exactly the reparametrization $\varphi_{ij} \mapsto \varphi_{ij} + \alpha_i + \beta_j$, and the alternating combination annihilates it, $\alpha_L + \beta_L + \alpha_R + \beta_R - \alpha_L - \beta_R - \alpha_R - \beta_L = 0$; four phases minus three independent local parameters leaves exactly one invariant, which is why φ_{ent} is the sole one rather than merely a convenient one. Third, W depends on the state only through φ_{ent} and through phases the first two steps remove, so it inherits both invariances.

The operational content is an integer. Tilly et al. [66] put the parallel two-branch geometry at $O(10^3)$ measurements to reject the no-entanglement hypothesis at 99.9% confidence in the near-zero-decoherence limit; that integer is the same integer computed in A's frame, where the masses are not the entangled pair and the laboratory is. A shot count, a fringe visibility and a spin correlator are QRF scalars; "A and B became entangled" is not. That asymmetry is the whole content of Section 5.

4.3 What the covariance does not license

Our proof runs on the translation subgroup with ideal frames, and both restrictions bite. The general-group construction of de la Hamette and Galley [25] and the perspective-neutral extension of de la Hamette et al. [26] show the formalism reaches much further; the boost case [37], the Lorentz case [7] and the superposed-geometry case [43] are worked out, but Table 1 is not proved for any of them, and carrying our conclusion there is speculative until the corresponding negativities are computed. Ideality is the sharper restriction: Palmer et al. [53] prove that a genuinely quantum frame change induces decoherence on the system described, Bartlett et al. [10] show a finite directional frame wears out after a number of high-precision uses scaling as N^2 in its size, and Höhn and Vanrietvelde [42] find a genuine discontinuity in the relational dynamics across a clock switch. A perfectly clean jump is an idealization we have used and should not be read as a claim about a real apparatus.

The three-body bookkeeping carries its own technical warning. Reduced states of a bystander after a QRF jump are not given by the naive partial trace, and Krumm et al. [45] supply the relational trace that is; their own stated scope is finite Abelian groups, which covers the translation model here and nothing wider.

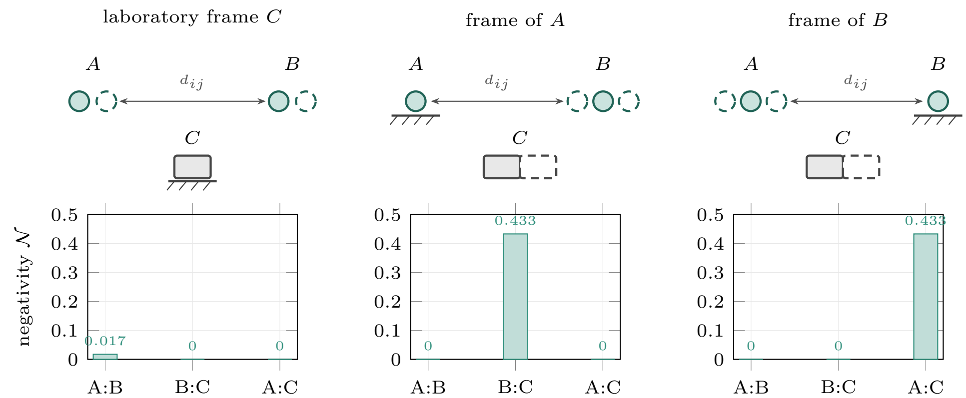

Figure 1: The same experiment drawn in three quantum reference frames, with the bipartite negativities of Table 2 beneath each: solid and dashed copies mark a body's two branches, the hatched symbol marks the body that is the frame, and the laboratory $\mathcal{N}_{AB}$ bar is evaluated at the worked point $\varphi_{\text{ent}} = -6.92 \times 10^{-2}$ rad, where it is 0.017 against the $\sqrt{3}/4 = 0.433$ the other two frames carry. All nine entries are recomputed in Appendix C.

Nor is the reshuffling itself a surprise once it is placed. That a tensor-product structure — and therefore which parties count as entangled — is induced by the accessible observables rather than given in advance is the observable-induced-partition result of Zanardi [72] and Zanardi et al. [73], pushed to its limit by Harshman and Ranade [40], who construct observables making any pure state carry any entanglement value one likes. Proposition 2 is a physically motivated instance of that general fact, not an exception to an otherwise absolute notion, and we claim novelty only for the computation and for pairing it with Proposition 3.

Frame-relativity of entanglement also predates the QRF program, and the precedents are adjacent rather than identical. Peres and Terno [56] and Peres et al. [55] establish that a reduced spin state is not Lorentz covariant and spin entropy has no invariant meaning; Gingrich and Adami [38] show spin and momentum entanglement trade against each other under a boost while the total is preserved. Those are Wigner-rotation effects in which a boost mixes internal and external degrees of freedom of the same particle, a different mechanism from a translation between distinct physical bodies, and treating them as the same phenomenon would be an analogy we decline; we cite them for the general claim that entanglement-adjacent quantities are frame-relative, and for the fact that the claim is old. Foo et al. [29] come closest to the present result, arguing that superposed amplitudes differing by a coordinate transformation can be re-expressed on one fixed background so that the associated decoherence depends on which external systems define the relative coordinates. Their "frame" is a coordinate relabelling and ours is a physical reference body, so the resemblance is structured rather than exact; we record it as a contested reading and rest nothing on it. The orientation degree of freedom that a closed loop of frames refuses to forget is developed in Corbeel [22], and the interferometer-as-clock-comparison identity that motivated this series' treatment of phase as the invariant object is Corbeel [21].

5 A positive result certifies a scalar, and "gravity entangled A with B" is not one

Section 4 leaves a successful run in an awkward reporting position. The measured witness is a quantum-reference-frame scalar fixed by the single combination φ_{ent}; the entanglement usually offered as its explanation is not, since the frame change that renders mass A definite moves the branch structure onto the pair (B, C) and redistributes the three bipartite negativities $\mathcal{N}$ tabulated in Appendix A and drawn in Fig. 1. Both statements are exact inside the translation-group model, and together they force a decision about which sentence the experiment is entitled to publish.

Proposition 4 (What a positive result certifies; structured, argued)**.** *The frame-invariant content of $W \neq W_{\text{classical}}$ is: no LOCC channel between the branch sectors reproduces the correlations, in any QRF — the gravitational interaction is nonclassical in the invariant sense. The frame-dependent content is any sentence of the form "gravity entangled A with B".*

The grading is structured at one joint, isolated here before the proposition is used: converting Section 4's exact invariance of W into a claim about the *content of an inference* imports premises the model does not contain, and those premises are what the published objections dispute. What follows restates the Marletto–Vedral claim invariantly, sorts the objections by which half of Proposition 4 they attack, and shows one prominent dispute half dissolved and half untouched.

5.1 The invariant restatement keeps the inference and drops the party names

The founding claims all name objects. Bose and collaborators state that “two objects cannot be entangled without a quantum mediator” [13]; Marletto and Vedral argue that gravitationally induced entanglement between two massive particles is *sufficient*, though not necessary, evidence of quantum effects in gravity [47], and later generalize the step beyond quantum theory, deriving on information-theoretic principles that any system able to mediate the local generation of entanglement between two quantum systems must itself be non-classical [48]. Marshman, Mazumdar and Bose ground the same witness in virtual graviton exchange and make microcausality the load-bearing premise explicitly [49].

Our restatement replaces the named pair with the branch sectors, and the replacement is exact within the model: the branch-pair distances d_{ij} are relative quantities, so each φ_{ij} and therefore $\varphi_{\rm ent}$ is fixed under the model's QRF group (Section 4), while the tensor factorization into A and B is not carried through the frame change at all. The sectors labeled $i, j \in \{L, R\}$ survive the jump because relational configuration data define them rather than a choice of subsystem, and the LOCC-impossibility statement quantifies over channels between them.

That the partition is the negotiable object here is no peculiarity of gravity. Which subsystems a state is entangled across is set by the operationally accessible observables rather than by particle labels [72, 73], and Harshman and Ranade give the sharpest version: for a fixed pure state, observables can be tailored to induce a tensor-product structure under which it takes essentially any entanglement value [40]. Reading Section 4's reshuffling as a physically forced instance of that freedom is a structured step rather than an exact one, since the QRF jump selects one repartition for a physical reason where those theorems establish only that repartitions exist. It places our computation inside an existing literature: entanglement-adjacent quantities were already not Lorentz scalars [38, 56], and states were already relational [36, 60].

The restatement also changes which null hypothesis the statistics reject, and that is where it earns its keep. Tilly, Marshman, Mazumdar and Bose find that the parallel two-branch geometry needs $O(10^3)$ measurements to reject the no-entanglement hypothesis at 99.9% confidence at near-zero decoherence, rising to $O(10^6)$ once the decoherence rate exceeds 0.125 Hz, where a six-dimensional qudit encoding becomes the optimum instead [66]. In the lab frame the two nulls — “the joint state is separable across $A : B$” and “some LOCC channel between branch sectors accounts for the correlations” — are rejected by the same data at the same confidence, exactly, since W and $\mathcal{N}$ are both functions of $\varphi_{\rm ent}$ alone. Only the second null still means anything after the frame change.

5.2 Almost every published objection attacks the invariant half, and frame-covariance does not help it

The classical-channel objections contest the inference, not the bookkeeping. Hall and Reginatto show the entanglement-implies-nonclassical-mediator step requires the additional premise that quantum systems cannot be entangled by a purely classical interaction, which holds for Koopman-type dynamics but fails in general, and they construct a configuration-ensemble classical model in which a classical mediator does entangle [39]. Trillo and Navascués sharpen this from the model side: the Diósi–Penrose theory of classical gravity predicts gravitationally induced entanglement whenever the separation falls below a critical distance proportional to the model's single free parameter, and in a geometry allowing perpendicular spreading that entanglement can survive for more than a day at reasonable experimental parameters [67]. Struyve proves the opposite for a neighboring family, showing that the Newton–Schrödinger model, its Bohmian analogue and the interpolating construction generate no entanglement at all in the same setup [64]. “Classical gravity” is therefore not one hypothesis, and the signature discriminates against one family while a second reproduces it; we report that as the state of the literature rather than as a result of ours.

The structural objections are stronger still. Galley, Giacomini and Selby prove, theory-independently, that three statements are jointly incompatible: that gravity can generate entanglement between two systems, that gravity mediates the interaction rather than the systems coupling directly, and that gravity is classical [33]. That is a trilemma about which premise fails, not a proof that gravity is quantum, and Di Biagio locates the premise the no-go theorems smuggle in — their locality assumption is information-theoretic rather than spatiotemporal, a sense in which quantum electrodynamics and perturbative quantum gravity already fail to be local, so detection of the effect alone cannot exclude classical gravity and discrimination requires quantitative comparison of low-energy predictions [28]. Fragkos, Kopp and Pikovski make the adjacent point that relativity does not dictate a local channel, so mediator and non-local descriptions of the same entanglement generation are equally available [30].

Anastopoulos and Hu's objection deserves its full force stated in our own notation: gravity-induced entanglement by Newtonian forces is agnostic to the quantum or classical nature of the gravitational true degrees of freedom [5]. Nothing in Section 2's derivation of $\varphi_{\rm ent}$ from $\varphi_{ij} = G m_A m_B t/(\hbar d_{ij})$ mentions a graviton; the quantity we prove invariant is an invariant of a Newtonian phase, and Proposition 4 does not repair that.

Their comment is an arXiv preprint whose v1 is the citable text and which was never accepted as a formal Comment, the weakest provenance of any source cited here, and it is nonetheless the objection our restatement least disturbs. The answers run on the same invariant terrain: Belenchia, Wald and collaborators argue from causality that the field of a superposed source must itself be able to carry quantum information [11, 12]; Martín-Martínez and Perche show a field-theoretic treatment produces the entanglement from linearized weak-field gravity, weakening the step from observation to graviton [50]; Christodoulou and Rovelli read the effect covariantly as a superposition of proper times, hence of geometries [20]. Every objection and every answer here would read identically if entanglement were a QRF scalar — an exact observation about their logical form, and a structured claim about their force: sorting them does not settle them.

5.3 The mediator dispute dissolves in half, and we say which half

The dispute worth naming is whether the entanglement is locally mediated by the gravitational field or is equally describable as a direct non-local process, with Marshman, Mazumdar and Bose on the mediation side [49], Fragkos, Kopp and Pikovski denying that relativity forces the choice [30], and Christodoulou and collaborators answering with a manifestly Lorentz-invariant path-integral derivation from linearized quantum gravity that exhibits retarded entanglement generation [19]. The disputed sentence "the field carried the entanglement from A to B" presupposes that the entanglement between A and B names a frame-independent quantity. Section 4 shows it does not, already in a three-body Newtonian model containing no field party whatsoever. To that extent the dispute is a dispute about bookkeeping relative to a frame, which is a structured conclusion; extending it to a genuine field mediator is speculative, since a field is not a system in the translation-group model and the general-group machinery that would admit one has been developed elsewhere [25].

What does not dissolve is retardation. Whether the correlations track the light cone is a property of the time dependence of φ_{ent}, not of any partition, and it is invariant in the same sense W is — structured, since we have not computed it in our model and this is a claim about what that computation would show, and further weakened by the authors' own note that their sharper retardation test is more readily realized in the electromagnetic analogue than in the gravitational case [19]. The half of the dispute asking which subsystems own the entanglement is a frame question; the half asking whether the correlations propagate is not, and remains decidable.

Lami, Pedernales and Plenio supply the cleanest independent evidence that the entanglement sentence was never carrying the certificate's weight: their LOCC inequality bounds how well any local-operations-and-classical-communication protocol can mimic gravitational unitary evolution of two oscillators in coherent states, and violating it certifies nonclassicality in a scheme where entanglement "is never created at any point" [46]. Theirs being a different witness makes the support structured rather than exact, and the same caution governs Foo, Mann and Zych's argument that decoherence attributed to superposed geometries related by a coordinate transformation is an artifact of the external systems fixing the relative coordinates [29]: their "frame" is a coordinate relabeling, ours a physical reference body, and the two must not be merged. Certifying a non-classical *causal order* from a mass superposition is the structurally parallel case, reporting an operational invariant rather than a subsystem fact [75]; the orientation dependence of a frame choice we treat separately [22].

The consequence is a change of wording in the result line, not of apparatus. The consortium roadmap states its aim as revealing gravitationally induced entanglement between two nanodiamond crystals [15], and the review literature keeps the same party-naming vocabulary [14]. The invariant report costs nothing experimentally: measure φ_{ent}, publish W, claim the LOCC-impossibility statement every frame in the model agrees on. Section 6 carries that quantity into the decoherence budget, where the threshold an experiment must beat is likewise a statement about φ_{ent} and not about who is entangled with whom.

6 Decoherence costs visibility, not invariance, which is what turns the split into a design tool

The distinction defended in Sections 4 and 5 would be bookkeeping if the invariant it isolates were the fragile half of the experiment. It is the durable half. Branch dephasing, the threat every parameter scan in this family budgets against [13, 47, 62], is a local channel on each mass's branch degree of freedom, and a local channel acts on the state, never on the unitary that prepared it. The combination φ_{ent} is a property of that unitary — four relational distances, a mass product and a time — so nothing the environment learns about which path a mass took can change it. What the environment takes is contrast, and contrast enters as a prefactor.

Proposition 5 (Robustness bound; exact within the model)**.** *With branch dephasing rate γ acting on either mass, the witness degrades as $W(\gamma)$ with the invariant φ_{ent} unchanged: the interference terms acquire the exact* *visibility factor $e^{-\gamma t}$, so that*

$$W(\gamma) \;=\; e^{-\gamma t}\, W(0), \qquad W(0) \;=\; f(\varphi_{\rm ent}), \quad f(\phi) = \phi + O(\phi^3), \tag{9}$$

for both witness forms of Appendix B, and the resulting detection threshold at significance z from N shots is

$$\varphi_{\rm ent}^{\rm min}(\gamma t, N) \;=\; \frac{z\, e^{\gamma t}}{\sqrt{N}}\, \big[1 + O(\varphi_{\rm ent}^2)\big]. \tag{10}$$

The algebra sits in Appendix B: dephasing in the branch basis multiplies every density-matrix element connecting distinct branches of a dephased mass by $e^{-\gamma t}$, each witness form of Section 2 is a sum of such elements, and a ± 1-valued correlator from N shots has standard error no worse than $N^{-1/2}$, so imposing $e^{-\gamma t} f(\varphi_{\rm ent}) \geq zN^{-1/2}$ gives (10). Two consequences should be kept apart. Every bipartite negativity $\mathcal{N}$ of Section 4 falls monotonically under the channel — exact, since negativity is an entanglement monotone under local operations — so decoherence erodes the covariant structure and the invariant's measurable shadow by different routes: the structure because the state degrades, the shadow only because contrast does. And γ enters (10) solely through γt, the one place a designer has anything to trade.

6.1 The figure of merit an apparatus must beat is a ratio of two rates

Proposition 5 becomes an optimization once Proposition 1's phase is read as a rate. Each $\varphi_{ij} = G m_A m_B t/(\hbar d_{ij})$ is linear in t, so

$$\varphi_{\rm ent} = \kappa t, \qquad \kappa = \frac{G m_A m_B}{\hbar} \left(\frac{1}{d_{LL}} + \frac{1}{d_{RR}} - \frac{1}{d_{LR}} - \frac{1}{d_{RL}} \right), \tag{11}$$

and the significance accumulated by the measurement is $S = \sqrt{N}\, \kappa t\, e^{-\gamma t}$ to leading order in $\varphi_{\rm ent}$. At fixed shot count S peaks at $t^\star = 1/\gamma$ with $S_{\max} = \sqrt{N}\, \kappa/(e\gamma)$; at fixed wall-clock budget $T = Nt$, where longer runs buy fewer of them, $S = \sqrt{T}\, \kappa\, \sqrt{t}\, e^{-\gamma t}$ and the optimum halves to $t^\star = 1/(2\gamma)$. Both are exact arithmetic on (10) and (11), and the factor of two is the gap between two hold times a proposal might quote for one apparatus. Either way the apparatus enters through a single dimensionless number, since detection at significance z requires $\kappa/\gamma \geq ez/\sqrt{N}$. Mass, geometry and screening act only on κ; vacuum, vibration and low-frequency Newtonian noise act only on γ. Proposition 3 makes κ a QRF scalar; whether γ is one is settled by nothing we have proved.

Published designs sit nowhere near $t^\star$, and saying so is the useful part. The screened QGEM scan tolerates a decoherence rate near 10^{-3} Hz for test masses of 10^{-14} kg at separations of about 35 μm, against roughly 450 μm unscreened [62]; at that rate $t^\star$ is of order 10^3 s, three orders beyond the sub-second interferometer times those geometries assume and some nine beyond the 7.6 μs motional coherence time of the first levitated nanoparticle cooled to its motional ground state [27] — structured, since trapped motional coherence and free-fall branch dephasing are not the same quantity. So Proposition 5's content in that regime is negative and worth stating: with $\gamma t \lesssim 10^{-3}$ the visibility factor departs from unity by less than a part in a thousand, so fringe loss is not what limits these designs. Dephasing binds as a ceiling on t, not as a discount on W.

The one scan that reports the crossover directly agrees with (10) under a structured reading. Tilly and collaborators require $O(10^3)$ measurements at 99.9% confidence with near-zero decoherence and $O(10^6)$ once the rate exceeds 0.125 Hz, where a six-branch encoding becomes optimal [66]. A thousand-fold rise in N at fixed $\varphi_{\rm ent}$ corresponds to $e^{2\gamma t} \approx 10^3$, that is $\gamma t \approx 3.5$, a hold time near 28 s at their crossover rate; since nothing in this family holds branches for 28 s, most of their jump is carried by the encoding change and not by visibility — a consistency check, not a rederivation. Optimizing κ/γ is the subject of the fourth paper in this series; its numerator already has demonstrated levers, since optimal-control expansion of a levitated wavepacket [70] and the measured threefold gain in motional coherence length [59] both act on the d_{ij} differences in (11), while the denominator is where a consortium-scale effort expects to spend, on vibration and gravitational-noise suppression [15, 61].

6.2 What we have not proved, and what would decide it

The honest boundary is that γ may not be the scalar κ is. A dephasing rate is fixed by a system–environment cut and by the monitored basis, both description-relative rather than given [73, 74]. Dephasing acting "on A" in the lab frame acts, after the jump to A's frame, on relational coordinates shared with B and C; calling that one process in new words is structured, not exact, since reducing onto a spectator after a frame change needs the relational trace rather than the naive partial trace [45]. Our frames are also ideal. A frame realized by a finite body induces decoherence on what it describes when it is switched [53] and wears out with use, the number of high-precision measurements against an N-spin directional frame scaling as N^2 [10] — a laboratory body is a depletable resource, and Propositions 2 and 3 assume it is not. The sharpest picture of a decoherence that is not a matter of description is the horizon-record mechanism, whose worked electromagnetic example gives about five minutes just outside a solar-mass horizon against 10^{43} years at one astronomical unit [24]; treating that as the invariant floor under laboratory γ is speculative, and we assert only the analogy. Collapse-model decoherence, which would suppress the signal across the model's whole parameter space [58], leaves $\varphi_{\rm ent}$ untouched as well.

Three things would decide the framework. Repeating Section 4's table for the Euclidean and Galilei groups, and later for superposed geometries, tests whether

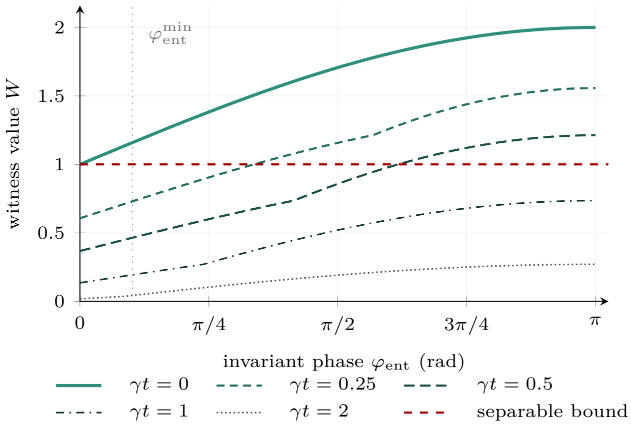

Figure 2: The setting-optimal witness of Appendix B against the invariant phase, for the branch-dephasing family $\gamma t \in \{0, 0.25, 0.5, 1, 2\}$; dephasing rescales the curve without moving $\varphi_{\rm ent}$, and the family crosses the separable bound only while $\gamma t < \ln 2$. The dotted rule is the detection threshold $\varphi_{\rm ent}^{\rm min}$ at $N = 10^3$ shots and $z = 3.09$; values are computed in Appendix C.

Proposition 3 survives a non-commuting group; its proof uses only the relational character of the d_{ij}, so we expect survival — speculative until computed [7, 25, 34, 43]. Whether a witness that creates no entanglement at any point — the LOCC inequality of Lami et al. [46] — is also a QRF scalar tests whether the invariant line is drawn in the right place; if it is not, the line is wrong. And Proposition 3 is falsifiable in the ordinary way: every frame in the model's group must report the same W at fixed $\varphi_{\rm ent}$, so a witness value depending, beyond statistics, on which physical body fixed the coordinates would refute it, and entangled clocks used as frames are the nearest proposed setting in which to look [17]. Companion papers in this series take the clock-comparison [21] and frame-orientation [22] faces of the same question.

What a successful run will establish, then, is a number rather than a story about two masses. The number is $\varphi_{\rm ent}$, reported through W, and its nonclassicality claim is the LOCC-impossibility statement the no-go trilemma constrains [33]; the story is frame-relative, and Fig. 2 shows the whole measurable family collapsing onto that one axis, with $e^{-\gamma t}$ setting only the vertical scale. Designers need the number, and (10) prices it: build an apparatus whose gravitational phase-accumulation rate exceeds its dephasing rate by $ez/\sqrt{N}$, and the frame question never has to be answered to publish the result.

A The three-frame algebra, worked

This appendix supplies the three results the main text uses without deriving: the negativity quoted in Proposition 1, the frame-changed states and the negativity table of Section 4, and the proof of Proposition 3. Everything below is exact algebra inside the model fixed in Section 3 — one spatial dimension, three bodies, ideal frames, orthogonal branch kets, and gravity as a c-number potential on relative configuration. Where a step leaves that model we say so in the sentence that takes it.

A.1 The normal form fixes $\varphi_{\rm ent}$ as the only surviving phase

Write the state of Proposition 1 with its coefficients exposed,

$$|\Psi\rangle = \tfrac{1}{2} \sum_{i,j\in\{L,R\}} e^{i\varphi_{ij}} \, |i\rangle_A |j\rangle_B, \qquad \varphi_{ij} = \frac{G\, m_A m_B\, t}{\hbar\, d_{ij}}, \tag{12}$$

abbreviate the coefficients as $c_{ij} = \frac{1}{2} e^{i\varphi_{ij}}$, and set $\varepsilon_L = +1$, $\varepsilon_R = -1$, $s_{ij} = \varepsilon_i \varepsilon_j$.

Lemma 1 (Normal form; exact)**.** *Every assignment of four phases φ_{ij} decomposes as $\varphi_{ij} = a_i + b_j + s_{ij}\,\varphi_{\rm ent}/4$ with $\varphi_{\rm ent} = \phi_{LL} + \phi_{RR} - \phi_{LR} - \phi_{RL}$, the pair (a_i, b_j) being determined up to the shift $a_i \to a_i + c$, $b_j \to b_j - c$. Consequently the local unitaries $U_A = \sum_i e^{-ia_i} |i\rangle\langle i|$ and $U_B = \sum_j e^{-ib_j} |j\rangle\langle j|$ carry $|\Psi\rangle$ to*

$$|\tilde\Psi\rangle = \tfrac{1}{2} \Big[e^{i\varphi_{\rm ent}/4} \big(|LL\rangle + |RR\rangle\big) + e^{-i\varphi_{\rm ent}/4} \big(|LR\rangle + |RL\rangle\big) \Big], \tag{13}$$

and no product unitary removes $\varphi_{\rm ent}$.

Proof. Substituting the decomposition into $\phi_{LL} + \phi_{RR} - \phi_{LR} - \phi_{RL}$ cancels every a_i and every b_j and leaves $4 \times \varphi_{\rm ent}/4$, so the decomposition is consistent; the map $(a_L, a_R, b_L, b_R) \mapsto (a_i + b_j)$ has a one-dimensional kernel, the stated shift, and a three-dimensional image inside the four-dimensional space of phase assignments, so the quotient is one dimensional and $\varphi_{\rm ent}$ spans the annihilator of the image. Since $U_A \otimes U_B$ shifts φ_{ij} by exactly $-a_i - b_j$, it can reach Eq. (13) and can reach nothing beyond it. □

The negativity follows from the normal form without further input. The concurrence of a two-qubit pure state is $2|c_{LL}c_{RR} - c_{LR}c_{RL}|$, and here

$$2|c_{LL}c_{RR} - c_{LR}c_{RL}| = \tfrac{1}{2} \big| e^{i(\phi_{LL}+\phi_{RR})} - e^{i(\phi_{LR}+\phi_{RL})} \big| \tag{14}$$

which, by $|e^{i\alpha} - e^{i\beta}| = 2|\sin[(\alpha - \beta)/2]|$, equals $|\sin(\varphi_{\rm ent}/2)|$. Writing the Schmidt weights as p and $1-p$, a pure bipartite state has partially transposed spectrum $\{p,\, 1-p,\, \pm\sqrt{p(1-p)}\}$, so that with $\mathcal{N}(\rho) = \frac{1}{2}(\|\rho^{T_B}\|_1 - 1)$ the negativity is $\sqrt{p(1-p)}$, which is half the concurrence. Hence

$$\mathcal{N}_{A:B} = \tfrac{1}{2} \big| \sin(\varphi_{\rm ent}/2) \big|, \tag{15}$$

the value quoted in Proposition 1. Every step here is exact.

A.2 The parallel geometry turns the invariant into one number

Fix the branch positions relative to C as $x_A \in \{-\Delta/2, +\Delta/2\}$ and $x_B \in \{d_0 - \Delta/2,\, d_0 + \Delta/2\}$, both masses split by the same Δ along the axis joining them — the parallel configuration the proposals assume. Then $d_{ij} = x_B^{(j)} - x_A^{(i)}$ gives

$$d_{LL} = d_{RR} = d_0, \qquad d_{LR} = d_0 + \Delta, \qquad d_{RL} = d_0 - \Delta, \tag{16}$$

and the invariant collapses to

$$\begin{aligned}\varphi_{\text{ent}} &= \frac{G m_A m_B t}{\hbar}\left[\frac{2}{d_0} - \frac{1}{d_0+\Delta} - \frac{1}{d_0-\Delta}\right] \\ &= -\frac{2 G m_A m_B t}{\hbar}\,\frac{\Delta^2}{d_0\,(d_0^2-\Delta^2)},\end{aligned} \tag{17}$$

which for $\Delta \ll d_0$ is $-2Gm_A m_B t\,\Delta^2/(\hbar d_0^3)$. The degeneracy $d_{LL} = d_{RR}$ is what makes φ_{ent} second order in Δ, and it is also what fixes the frame-changed alphabet below, so the two facts the paper cares about have one source.

One arithmetic illustration, ours and not a measurement. Reading the unscreened QGEM design point of Schut and Mazumdar [62] — test masses of 10^{-14} kg, separation 450 μm, superposition size 200 μm — as $m_A = m_B = 10^{-14}$ kg, $d_0 = 450$ μm and $\Delta = 200$ μm is a structured identification of their quoted numbers with our symbols rather than an exact one, since their separation figure is a design requirement and not a centre-to-centre coordinate. On that reading the bracket in Eq. (17) is -1.09×10^3 m^{-1} and $Gm_A m_B/\hbar = 6.33\times10^{-5}$ m s^{-1}, so an interaction time of one second — our choice of operating point, made to fix ideas — gives $|\varphi_{\text{ent}}| = 6.9\times10^{-2}$ and, through Eq. (15), $\mathcal{N}_{A:B} = 1.7\times10^{-2}$. The arithmetic is exact given the identification; the identification is the part to check.

A.3 The frame change moves the branch structure onto the spectator

Apply the map of Eq. (5) to Eq. (12). On branch kets $|a_i\rangle_A|b_j\rangle_B \mapsto |-a_i\rangle_C|b_j - a_i\rangle_B$, and since each basis ket goes to a basis ket the amplitude $\frac{1}{2}e^{i\varphi_{ij}}$ rides along untouched. With the geometry of Eq. (16) the relative positions $b_j - a_i$ take the three values $d_0 - \Delta$, d_0 and $d_0 + \Delta$, the middle one twice, so

$$\begin{aligned}|\Psi\rangle^{(A)} = \tfrac{1}{2}\Big[&|c_L\rangle_C\big(e^{i\phi_{LL}}|d_0\rangle_B + e^{i\phi_{LR}}|d_0+\Delta\rangle_B\big) \\ &+ |c_R\rangle_C\big(e^{i\phi_{RL}}|d_0-\Delta\rangle_B + e^{i\phi_{RR}}|d_0\rangle_B\big)\Big],\end{aligned} \tag{18}$$

with $|c_i\rangle = |-a_i\rangle$. Two features of Eq. (18) deserve naming. A has vanished as a system, because its position relative to itself is zero; and B's alphabet has grown from two orthogonal kets to three, because "where B can be found" is referred to an origin that is itself spread over two places. In the continuum description on $L^2(\mathbb{R})\otimes L^2(\mathbb{R})$ the map is unitary [36]; restricted to the finite branch bases it is an isometry into a larger finite-dimensional subspace, and the growth of the alphabet is that isometry seen in the basis, not a creation of states. This is exact.

Reducing on C in Eq. (18) gives, in the basis $\{|c_L\rangle, |c_R\rangle\}$,

$$\rho_C^{(A)} = \begin{pmatrix} \frac{1}{2} & \frac{1}{4}e^{i(\phi_{LL}-\phi_{RR})} \\ \frac{1}{4}e^{-i(\phi_{LL}-\phi_{RR})} & \frac{1}{2}\end{pmatrix}, \tag{19}$$

because the only surviving cross term in the partial trace is the one pairing $|d_0\rangle$ with itself. Its eigenvalues are $\frac{1}{2}\pm\frac{1}{4}$, that is $\frac{3}{4}$ and $\frac{1}{4}$. The state in Eq. (18) is pure, so the Schmidt relation used for Eq. (15) applies and $\mathcal{N}^{(A)}_{B:C} = \sqrt{3}/4 \simeq 0.433$. The same computation in B's perspective, with $\hat{S}_{C\to B}$ and relative positions $a_i - b_j \in \{-d_0-\Delta, -d_0, -d_0+\Delta\}$, gives $\mathcal{N}^{(B)}_{A:C} = \sqrt{3}/4$ by the identical cross-term count.

Lemma 2 (The frame-changed negativity is blind to gravity; exact)**.** *In A's perspective, $\mathcal{N}^{(A)}_{B:C}$ is independent of every φ_{ij}, and hence of φ_{ent}. It equals $\frac{1}{2}$ when the four relative positions $b_j - a_i$ are distinct, and $\sqrt{3}/4$ when exactly one coincidence $b_j - a_i = b_{j'} - a_{i'}$ with $i \neq i'$ occurs, which is the case if and only if the two branch separations are equal.*

Proof. The off-diagonal element is $(\rho_C)_{LR} = \frac{1}{4}\sum_{j,j'} e^{i(\phi_{Lj}-\phi_{Rj'})}\langle b_{j'} - a_R|b_j - a_L\rangle$, in which only terms with $b_j - a_L = b_{j'} - a_R$ survive. Equality for $(j,j') = (L,R)$ requires $b_L - b_R = a_L - a_R$, and for $(j,j') = (R,L)$ requires $b_R - b_L = a_L - a_R$; with both splittings positive and co-oriented at most the first can hold, so the sum has either no surviving term or exactly one. If none, ρ_C is $\frac{1}{2}$ times the identity and $\mathcal{N} = \frac{1}{2}$. If one, the element is a single phase of modulus $\frac{1}{4}$, the eigenvalues are $\frac{1}{2}\pm\frac{1}{4}$ whatever that phase is, and $\mathcal{N} = \sqrt{3}/4$. In neither case does any φ_{ij} enter the spectrum. $\square$

Lemma 2 is the sharp form of the covariance claim, and it is sharper than "the entanglement moves." In A's perspective the surviving negativity is fixed by the coincidence pattern of the relative-position alphabet, which is geometry, and it is already $\sqrt{3}/4$ at $t=0$ when the lab-frame negativity is exactly zero. The lab frame's gravitational entanglement does not reappear in A's frame as a number one could read off; it is absorbed into a quantity whose value gravity does not touch. Reading that as vindicating rather than contradicting the informal expectation that "A:B entanglement appears partly as B:C entanglement" is a structured judgement on our part: the bipartition does move as expected, and what does not move is the gravitational information, which

Perspective	$\mathcal{N}_{A:B}$	$\mathcal{N}_{B:C}$	$\mathcal{N}_{A:C}$
laboratory body C	$\frac{1}{2}\lvert\sin(\varphi_{\mathrm{ent}}/2)\rvert$	0	0
mass A	0	$\sqrt{3}/4$	0
mass B	0	0	$\sqrt{3}/4$

Table 2: Bipartite negativities of the same experiment in three perspectives, equal branch separations, orthogonal branch kets. Each row has exactly one non-zero entry, pairing the two bodies that are not the frame. Only the first depends on gravity.

the proof of Proposition 3 below shows travels in φ_{ent} instead.

A.4 The table, and the six entries that make the point

Each perspective has a body that is definite in it, and a bipartition containing that body is a product with the rest of the description, so its negativity is zero — not undefined. Collecting Eqs. (15) and (19) and their B-frame counterpart gives Table 2, whose values are the ones Section 4 plots.

The six zeros carry the argument. A quantity is a QRF scalar when it takes the same value in every perspective, and $\mathcal{N}_{A:B}$ takes the value $\frac{1}{2}\lvert\sin(\varphi_{\mathrm{ent}}/2)\rvert$ in one perspective and 0 in two others, so it is not one. This is exact, and it is a physically forced instance of the general observable-induced relativity of subsystem structure [73] discussed in Section 3, rather than an anomaly of the gravitational case.

A.5 Proposition 3 in full

Proof of Proposition 3. Step 1, the group. The model's QRF group is generated by rigid translations $T(\xi) : x \mapsto x + \xi$ applied to all bodies, together with the frame-change isometries $\hat{S}_{C\to A}$, $\hat{S}_{C\to B}$, their inverses and their compositions, of which $\hat{S}_{A\to B} = \hat{S}_{C\to B}\hat{S}_{C\to A}^{-1}$ is representative. These are the translation-group QRF transformations of Giacomini et al. [36] and nothing else; boosts, rotations and clock changes are outside it by the scoping of Section 3.

Step 2, the distances are pointwise fixed. A rigid translation leaves every difference $x_B - x_A$ unchanged. Under $\hat{S}_{C\to A}$ the coordinates (x_A, x_B) become $(x'_C = -x_A,\ x'_B = x_B - x_A)$, so $x'_B - x'_C = x_B - x_A$: the separation between the two masses is the same function of the new coordinates as of the old. Hence every d_{ij} in Eq. (16), being a difference of positions of A and B, is invariant under the whole group, and by Eq. (12) so is every φ_{ij}, and a fortiori φ_{ent} — including its sign, which is a stronger statement than local-unitary invariance gives. Exact.

Step 3, the amplitudes ride along. Each generator carries branch kets to branch kets, so the coefficient $\frac{1}{2}e^{i\varphi_{ij}}$ attaches to the image ket unchanged, as Eq. (18) exhibits for $\hat{S}_{C\to A}$. The phase data readable off the state is therefore the same list in every perspective, even though the systems the list is indexed by are not. The internal registers on which the spin-witness form is measured are untouched, because the group acts on positions only; this is exact within the model and fails for any extension in which the frame change acts on internal degrees of freedom, as the relativistic constructions of Giacomini et al. [37] do.

Step 4, the witness is a function of φ_{ent}. By Lemma 1 the state is, up to local unitaries on the two branch registers, Eq. (13), whose only parameter is φ_{ent}. Any functional of the state invariant under those local unitaries is therefore a function of φ_{ent} alone, and in fact of $\lvert\sin(\varphi_{\mathrm{ent}}/2)\rvert$, since that is the complete local-unitary invariant of a two-qubit pure state; the negativity of Eq. (15) is the example. A witness W measured with fixed settings is not of that kind: it also depends on the removable phases a_i and b_j. But those are single-mass phases, fixed by the interferometer geometry and calibrated by running each arm with the other mass withdrawn, and both witness forms of Appendix B are evaluated with settings referred to that calibration. With the settings so referred, W is a function of φ_{ent}. The calibration step is an operational assumption, exact inside the model and worth naming because it is the one place where an experimenter's procedure, rather than the algebra, does the work.

Step 5. Combining Steps 2 and 4, W is a function of a quantity every element of the group leaves fixed, hence W is a QRF scalar. By Table 2, $\mathcal{N}_{A:B}$ is not. The two statements are consistent because $\mathcal{N}_{A:B}$ is a property of a bipartition and φ_{ent} is a property of the relational configuration, and only the second is available in every perspective. ☐

A.6 What the algebra assumes

Four idealizations carry the table. Branch kets are orthogonal: finite-width packets make $\langle d_0 | d_0 + \Delta\rangle$ nonzero, which moves the entries of Table 2 continuously and leaves Lemma 2's conclusion intact only in the limit of vanishing overlap, so the table's $\sqrt{3}/4$ is a limiting value and not a measured one. Frames are ideal: a frame change between physical quantum frames induces decoherence [53], which our isometries do not. Reduced states are taken inside each perspective's own reduced Hilbert space and never by tracing over the frame body, which is the operation Krumm et al. [45] show to be ill-defined for a third system; we follow the perspective-neutral prescription [69] instead. And gravity is a c-number potential on relative configuration throughout, so nothing here is a statement about a gravitational field with its own state. Each of these would have to be lifted separately, and we regard lifting the last as the one that could change the result rather than its numbers.

B Both witness forms, and what dephasing does to them

This appendix carries out the algebra Section 2 cites and Section 6 uses. It has four parts: a canonical form for the state of Eq. (2), an exact spectral decomposition of its correlation matrix, the evaluation of the fringe-correlation and spin-witness readouts on it, and the effect of branch dephasing on both together with the detection threshold that follows. Every step is exact within the two-branch truncation stated in Section 2; where a step imports a convention rather than deriving one, the sentence says so.

B.1 Canonical form

Lemma 3 (Canonical two-branch form)**.** *Set* $a_L = 0$, $a_R = \phi_{RL} - \phi_{LL}$, $b_L = \phi_{LL}$, $b_R = \phi_{LR}$. *The local phase gates* $\mathrm{diag}(e^{-ia_L}, e^{-ia_R}) \otimes \mathrm{diag}(e^{-ib_L}, e^{-ib_R})$ *map the state of Eq.* (2) *to*

$$|\tilde{\Psi}\rangle = \tfrac{1}{2}\left(|LL\rangle + |LR\rangle + |RL\rangle + e^{i\varphi_{\mathrm{ent}}}|RR\rangle\right). \qquad (20)$$

The three off-diagonal residuals vanish by construction, and the fourth is $\phi_{RR} - (a_R + b_R) = \phi_{RR} + \phi_{LL} - \phi_{RL} - \phi_{LR} = \varphi_{\mathrm{ent}}$ by Eq. (3). This is exact and is the operational content of Proposition 1's middle clause: a single controlled phase φ_{ent}, applied to an unentangled pair of equal-weight branch superpositions, reproduces the entire state up to operations either interferometer can perform on itself. The concurrence of Eq. (20) is $2|c_{LL}c_{RR} - c_{LR}c_{RL}| = |e^{i\varphi_{\mathrm{ent}}} - 1|/2 = |\sin(\varphi_{\mathrm{ent}}/2)|$, which reproduces the negativity $\mathcal{N} = |\sin(\varphi_{\mathrm{ent}}/2)|/2$ quoted in Proposition 1 and derived independently in Appendix A; the agreement of two routes is a check, not a second result.

B.2 The correlation matrix has a two-line spectral form

Write $|L\rangle, |R\rangle$ as the $+1, -1$ eigenvectors of σ_z, so that σ_z is the which-branch observable and any equatorial direction $\hat{a}(\alpha) = (\cos\alpha, \sin\alpha, 0)$ is the observable read by recombining that interferometer with offset α. Let $T_{mn} = \langle \sigma_m^A \otimes \sigma_n^B \rangle$ on Eq. (20). Direct evaluation gives

$$T = \begin{pmatrix} \cos^2(\varphi_{\mathrm{ent}}/2) & \frac{1}{2}\sin\varphi_{\mathrm{ent}} & \sin^2(\varphi_{\mathrm{ent}}/2) \\ \frac{1}{2}\sin\varphi_{\mathrm{ent}} & \sin^2(\varphi_{\mathrm{ent}}/2) & -\frac{1}{2}\sin\varphi_{\mathrm{ent}} \\ \sin^2(\varphi_{\mathrm{ent}}/2) & -\frac{1}{2}\sin\varphi_{\mathrm{ent}} & 0 \end{pmatrix}, \qquad (21)$$

which collapses, with $\hat{u} = (\cos(\varphi_{\mathrm{ent}}/2), \sin(\varphi_{\mathrm{ent}}/2), 0)$ and $\hat{v} = (\sin(\varphi_{\mathrm{ent}}/2), -\cos(\varphi_{\mathrm{ent}}/2), 0)$, to

$$T = \hat{u}\hat{u}^{\mathsf{T}} + \sin(\varphi_{\mathrm{ent}}/2)\left(\hat{z}\hat{v}^{\mathsf{T}} + \hat{v}\hat{z}^{\mathsf{T}}\right). \qquad (22)$$

Equation (22) is exact and does all the remaining work. It says that the state's correlations decompose into one perfectly correlated equatorial direction — the same direction $\hat{u}$ on both masses, tilted by half the invariant phase — plus a block of strength $|\sin(\varphi_{\mathrm{ent}}/2)|$ that pairs the which-branch axis on one mass with the orthogonal equatorial direction on the other. The singular values of T are therefore $\{1, |\sin(\varphi_{\mathrm{ent}}/2)|, |\sin(\varphi_{\mathrm{ent}}/2)|\}$, and since T transforms under local unitaries as $T \mapsto R_A^{\mathsf{T}} T R_B$ with R_A, R_B rotations, those three numbers are local-unitary invariants, as Proposition 1 requires.

B.3 The fringe-correlation readout cannot witness entanglement

Contract Eq. (22) with two equatorial settings. Since $\hat{a}(\alpha)\cdot\hat{u} = \cos(\alpha - \varphi_{\mathrm{ent}}/2)$, $\hat{a}(\alpha)\cdot\hat{v} = -\sin(\alpha - \varphi_{\mathrm{ent}}/2)$ and $\hat{a}(\alpha)\cdot\hat{z} = 0$, the second term drops entirely and

$$E(\alpha, \beta) = \hat{a}(\alpha)^{\mathsf{T}} T\, \hat{a}(\beta) = \cos\!\left(\alpha - \tfrac{\varphi_{\mathrm{ent}}}{2}\right)\cos\!\left(\beta - \tfrac{\varphi_{\mathrm{ent}}}{2}\right). \qquad (23)$$

The fringe correlator factorizes exactly, for every value of φ_{ent}, into one function of each interferometer's own recombination offset. An exactly factorizing correlator is reproduced by a product state — take Bloch vectors $\hat{u}$ on each mass — so no linear functional of equatorial-setting correlators alone can distinguish Eq. (20) from a separable state, at any φ_{ent}, including $\varphi_{\mathrm{ent}} = \pi$ where the state is maximally entangled. What the fringe readout does deliver is the phase itself, read off as the offset $\varphi_{\mathrm{ent}}/2$ at which each interferometer's fringe peaks; entanglement then follows by Proposition 1 rather than by measurement. This is an exact statement about this state and not a general one: a maximally entangled two-qubit state has orthogonal T, and here the unit singular direction happens to lie in the recombination plane on both sides, which is what starves the equatorial block. The practical consequence is the one Section 2 draws: a model-independent entanglement certification requires at least one which-branch reading, and the distinction between measuring φ_{ent} and witnessing entanglement is a real distinction, not a presentational one.

B.4 The spin-witness family, its bound, and its optimum

Consider the two-setting witness

$$W = \left|\langle \sigma_{\hat{a}}^A \otimes \sigma_{\hat{b}}^B \rangle + \langle \sigma_{\hat{c}}^A \otimes \sigma_{\hat{d}}^B \rangle\right|, \qquad \hat{a} \perp \hat{c}, \quad \hat{b} \perp \hat{d}, \qquad (24)$$

the family in which Bose et al. [13] cast the BMV certification. For a product state with Bloch vectors $\vec{r}_A, \vec{r}_B$ the expression inside the modulus is $(\vec{r}_A\hat{a})(\vec{r}_B\hat{b}) + (\vec{r}_A\hat{c})(\vec{r}_B\hat{d})$, which Cauchy–Schwarz bounds by $\sqrt{(\vec{r}_A\cdot\hat{a})^2 + (\vec{r}_A\cdot\hat{c})^2}\cdot\sqrt{(\vec{r}_B\cdot\hat{b})^2 + (\vec{r}_B\cdot\hat{d})^2} \le |\vec{r}_A|\,|\vec{r}_B| \le 1$, using orthogonality of each setting pair; the expression is linear in the state, so the bound survives convex mixing and $W \le 1$ for every separable state. The derivation is exact and takes three lines; we reproduce it because the rest of this appendix reads thresholds off it and a threshold whose provenance is not visible is not auditable.

The value of W depends on the settings as well as the state, and the two facts diverge sharply. With the fixed settings $(\hat{a}, \hat{b}, \hat{c}, \hat{d}) = (\hat{x}, \hat{z}, \hat{y}, \hat{y})$ in the canonical frame of Lemma 3, Eqs. (21) give

$$W_{\text{fix}} = |T_{xz} + T_{yy}| = 2\sin^2(\varphi_{\text{ent}}/2), \tag{25}$$

which exceeds unity only for $|\varphi_{\text{ent}}| > \pi/2$. Optimizing instead over settings, write the bracket as $\mathrm{Tr}(TM)$ with $M = \hat{b}\hat{a}^{\mathsf{T}} + \hat{d}\hat{c}^{\mathsf{T}}$; then $M^{\mathsf{T}}M = \hat{a}\hat{a}^{\mathsf{T}} + \hat{c}\hat{c}^{\mathsf{T}}$ is a rank-two projector, so M has singular values $\{1, 1, 0\}$ and von Neumann's trace inequality gives $W \leq s_1(T) + s_2(T)$, attained by taking $\hat{b}, \hat{d}$ the leading right singular vectors of T and $\hat{a}, \hat{c}$ the corresponding left ones. With the singular values read off Eq. (22),

$$W_{\max} = 1 + |\sin(\varphi_{\text{ent}}/2)| = 1 + 2\mathcal{N}, \tag{26}$$

exact, which exceeds unity for every $\varphi_{\text{ent}} \neq 0$. The gap between Eqs. (25) and (26) is not a detail: a fixed-setting witness is blind to the entire range $0 < |\varphi_{\text{ent}}| < \pi/2$, where $\mathcal{N}$ runs from 0 to 0.354, and closing that blindness costs nothing but a choice of measurement axes. Equation (26) is also the statement Section 4 needs for Proposition 1's last clause and for the invariance argument: the setting-optimal witness is a function of φ_{ent} alone, because the singular values of T are local-unitary invariants and the locally removable phases of Section 2 act on T exactly as local rotations.

B.5 Branch dephasing

Model decoherence as pure dephasing in the branch basis at rates γ_A, γ_B acting for the interaction time t: the channel's adjoint fixes σ_z and multiplies σ_x, σ_y by $\lambda_A = e^{-\gamma_A t}$ on mass A and $\lambda_B = e^{-\gamma_B t}$ on mass B. This is where the visibility factor enters, and it enters exactly once per equatorial index: $T_{mn} \mapsto \mu_m^A \mu_n^B T_{mn}$ with $\mu_x = \mu_y = \lambda$, $\mu_z = 1$. Because $\hat{u}$ and $\hat{v}$ are equatorial and $\hat{z}$ is not, Eq. (22) transforms without mixing:

$$T(\lambda_A, \lambda_B) = \lambda_A \lambda_B\, \hat{u}\hat{u}^{\mathsf{T}} + \sin(\varphi_{\text{ent}}/2)\left(\lambda_B\, \hat{z}\hat{v}^{\mathsf{T}} + \lambda_A\, \hat{v}\hat{z}^{\mathsf{T}}\right), \tag{27}$$

whose singular values are exactly

$$\{\lambda_A\lambda_B,\ \lambda_A|\sin(\varphi_{\text{ent}}/2)|,\ \lambda_B|\sin(\varphi_{\text{ent}}/2)|\}\,. \tag{28}$$

The invariant φ_{ent} is untouched — dephasing does not change the phase, only the amplitude with which correlations built on it survive — which is the precise sense in which Section 6's robustness statement holds. Writing $\lambda_A = \lambda_B = \lambda$ and $C = |\sin(\varphi_{\text{ent}}/2)|$, the setting-optimal witness is $W_{\max} = 2\lambda C$ when $C \geq \lambda$ and $\lambda C + \lambda^2$ otherwise, while the fixed settings of Eq. (25) degrade to $W_{\text{fix}} = \lambda(1+\lambda)\sin^2(\varphi_{\text{ent}}/2)$ — asymmetric, because a which-branch reading is immune to the dephasing that erases a fringe. Three exact consequences follow. The fixed-setting witness cannot exceed unity at any φ_{ent} once $\lambda(1+\lambda) < 1$, that is once $\gamma t > \ln\frac{1+\sqrt{5}}{2} = 0.481$. The setting-optimal witness cannot exceed unity once $2\lambda < 1$, that is once $\gamma t > \ln 2 = 0.693$, and no choice of geometry, mass, or interaction time moves that ceiling because it is saturated only at $C = 1$. And in the regime $C \geq \lambda$ the optimum $2\lambda C$ is attained inside the experimentally plain family that pairs a recombined reading on one mass with a which-branch reading on the other, at offsets $\alpha = \beta = \varphi_{\text{ent}}/2 - \pi/2$; tilted settings buy an advantage only in the low-dephasing corner $\lambda > C$, where they lift the requirement on φ_{ent} substantially.

B.6 The detection threshold

Estimate each of the two correlators in Eq. (24) from $N/2$ shots of ± 1 outcomes. At the optimum both equal $W/2$, so the summed estimator has variance $(4 - W^2)/N$ exactly, and rejecting the separable hypothesis at z standard deviations requires $W - 1 \geq z\sqrt{(4 - W^2)/N}$, i.e.

$$W \geq W_{\min}(N, z) = \frac{N + z\sqrt{3N + 4z^2}}{N + z^2}. \tag{29}$$

The Gaussian z-score reading of Eq. (29) is a convention imported from ordinary practice rather than derived here, and it is the one step in this appendix that is structured rather than exact: at small N the binomial tail is not Gaussian and Eq. (29) understates the required margin. Combining Eq. (29) with the dephased witness gives the quantity a designer needs,

$$\varphi_{\text{ent}}^{\min}(\gamma t, N) = 2\arcsin\left[\min\left\{W_{\min}e^{\gamma t} - e^{-\gamma t},\ \tfrac{1}{2}W_{\min}e^{\gamma t}\right\}\right], \tag{30}$$

where the first branch is the tilted-setting optimum and the second the recombination-plus-which-branch optimum, and where a real solution exists only for $\gamma t \leq \ln(2/W_{\min})$, tending to $\ln 2$ as $N \to \infty$. Three worked points, exact arithmetic on Eq. (30) at $z = 3.09$ (a one-sided 99.9% level): at $N = 10^3$ and $\gamma t = 0$, $W_{\min} = 1.159$ and $\varphi_{\text{ent}}^{\min}$ is 0.32 rad with tilted settings but 1.24 rad without them, a factor of 3.9 in required phase bought purely by the measurement axes; at $N = 10^3$ and $\gamma t = 0.3$ the threshold is 1.80 rad, the two branches having crossed at $\gamma t = 0.273$ (at 0.3 they read 1.94 and 1.80 rad, and the minimum governs); and at $N = 10^6$ the dephasing ceiling rises only from 0.545 to 0.688, because shots buy margin logarithmically slowly against an exponential. Tilly et al. [66] report, for the parallel two-qubit geometry at near-zero decoherence, that order 10^3 measurements suffice to reject the no-entanglement hypothesis at 99.9% confidence, rising to order 10^6 once the decoherence rate passes 0.125 Hz, above which six-branch qudit encodings become the better use of the same apparatus, and that grouping witness operators can cut the measurement count up to ten-fold. Our $N = 10^3$ point lands in the same place for a protocol run near maximal φ_{ent}; the agreement is structured rather than exact, since their witness construction, geometry family, and hypothesis test are not identical to Eq. (24), and a factor-of-a-few discrepancy in N would not distinguish the two treatments.

One reconciliation should be stated rather than left for a reader to notice. In the corner $\gamma t \to 0$, $N \to \infty$ the tilted-setting branch of Eq. (30) reduces to $\varphi_{\text{ent}}^{\min} \to 2\sqrt{3}\, z e^{\gamma t}/\sqrt{N}$, which is the $z e^{\gamma t}/\sqrt{N}$ scaling quoted at section level in Eq. (10), with the numerical prefactor $2\sqrt{3}$ supplied here by the separable bound and the exact estimator variance. Outside that corner the two expressions part company in a way that matters: because the test is distinguishability from $W = 1$ and not from $W = 0$, the exact threshold diverges at finite γt and no number of shots recovers detection past $\gamma t = \ln 2$, whereas a threshold written as a bare inverse square root in N carries no ceiling at all. Where the two disagree, Eq. (30) is the statement to design against; the section-level form is its small-phase, small-dephasing shadow.

B.7 What this model leaves out

Branch dephasing at a single rate is a stand-in, not a decoherence budget. It represents environmental monitoring of the which-branch degree of freedom in the einselection sense [74], and it does not represent the Continuous Spontaneous Localization dynamics that Rijavec et al. [58] find would hinder gravitationally induced entanglement across the whole of that model's parameter space — a modification of quantum mechanics, not a channel acting on ordinary quantum states, and therefore not obtainable by any choice of γ in Eq. (27). It also does not represent the decoherence Palmer et al. [53] show is induced by the act of changing between finite-resource quantum reference frames, which is a distinct effect and one that Section 3's idealization of perfect frames explicitly sets aside. Nor does the two-setting family of Eq. (24) exhaust what a laboratory could do: Chevalier et al. [18] show that a modified protocol reduces the required interaction time enough to tolerate higher decoherence rates and identify a loophole that only full state tomography closes, and Lami et al. [46] certify gravitational nonclassicality through a local-operations-and-classical-communication inequality on coherent states in which entanglement is never generated at any point — a witness outside this appendix's framework entirely, and one whose existence Section 5 takes seriously when it separates what a positive result establishes from what it is usually said to establish. The thresholds above are exact for the model stated and should be read as a floor on difficulty, never as a budget.

C Simulation method and full output

C.1 `sim_frames.py`

Everything this paper computes numerically is computed by one script, `sim_frames.py`, which requires `numpy` and nothing else, writes its own stdout to `sim_frames_output.txt` and its machine-readable results to `sim_frames_output.json`, and produces byte-identical files on a second run. Run it with `python3 sim_frames.py` from the paper directory. The one declared seed, `20260919`, is passed to `numpy.random.default_rng` and is used by exactly one computation — the twenty thousand random phase quadruples on which block (a) tests Eq. (15) against a numerical partial transpose — so no physical number printed here depends on it. The rest is closed-form arithmetic on the two constants §2 prints, $G = 6.674 \times 10^{-11}\,\mathrm{m^3 kg^{-1} s^{-2}}$ and $\hbar = 1.0546 \times 10^{-34}\,\mathrm{J\,s}$, and on the QGEM geometries §2, §4 and Appendix A cite.

The script runs in three blocks, one per figure element. Block (a) builds the state of Eq. (2) at the two worked operating points, takes its negativity from the eigenvalues of the partial transpose of $|\Psi\rangle\langle\Psi|$, and checks that number against the closed form of Eq. (15) there and on a swept and a seeded family of phase assignments; the laboratory value it returns is the first bar of Fig. 1. Block (b) applies the frame maps of Eq. (5) in the branch-basis form Eq. (18) writes, and computes all nine entries of Table 2 from one partial-transpose routine; those nine numbers are the three bar triples of Fig. 1. Block (c) evaluates both witness forms of Appendix B across the dephasing family $\gamma t \in \{0, 0.25, 0.5, 1, 2\}$ together with the thresholds of Eqs. (29) and (30); its curves are the ones Fig. 2 draws. Both figure bodies carry the sampled coordinates literally, so no figure reads a file at build time, and nothing in either figure was drawn by hand.

Three conventions are fixed by the script rather than by the prose, and each is printed where it is used. First, two operating points carry the whole of block (a): point U, the unscreened geometry $d_0 = 450\,\mu\mathrm{m}$, $\Delta = 200\,\mu\mathrm{m}$ that Appendix A works, and point S, the screened geometry $d = 35\,\mu\mathrm{m}$, $\Delta = 1\,\mu\mathrm{m}$ that §4 works, both at $m_A = m_B = 10^{-14}\,\mathrm{kg}$ and at the one-second interaction time Appendix A declares as the paper's own choice; every phase printed is linear in that time, so a reader who prefers another hold rescales rather than recomputes. Second, orthogonal branch kets are implemented literally as one basis vector per distinct relative position, positions being identified at picometre resolution. That is what makes B's alphabet three-dimensional in A's perspective and four-dimensional when the arms are unequal, and the printout records the dimension triple $(\dim A, \dim B, \dim C)$ for every perspective so that the alphabet growth of Eq. (18) is visible rather than asserted. Third, a bipartition containing the frame body is computed and not assumed: the frame carries a one-dimensional factor, the partial trace and the partial transpose run across it exactly as they run across any other, and the six zeros of Table 2 come out of the same routine that returns the two non-zero entries. That makes the zeros auditable, which is the only reason to spend arithmetic on a quantity the convention of §4 already fixes.

Full stdout follows, reproduced verbatim from `sim_frames_output.txt`.

```
sim_frames.py -- SY-A03, How Much of Gravitationally
Induced Entanglement Is in the Eye of the Frame
deterministic; numpy only; seed = 20260919
========================================================
CONSTANTS AND WORKED PARAMETERS
  G      = 6.674e-11 m^3 kg^-1 s^-2   [Sec. 2 text]
  hbar   = 1.0546e-34 J s             [Sec. 2 text]
  m_A = m_B = 1e-14 kg                [Sec. 2, QGEM]
  t      = 1 s (illustrative hold)    [App. A]
  z      = 3.09 (one-sided 99.9%)     [App. B]
  point U, unscreened QGEM            [App. A]
    d_0 = 450 um, Delta = 200 um
  point S, screened QGEM              [Sec. 4]
    d_0 = 35 um,  Delta = 1 um
  G m_A m_B / hbar = 6.3285e-05 m s^-1
========================================================
(a) BMV STATE, INVARIANT PHASE, NEGATIVITY
--------------------------------------------------------
|Psi> = 1/2 sum_ij exp(i phi_ij) |i>_A |j>_B
phi_ij = G m_A m_B t / (hbar d_ij)   [Eq. (bmvstate)]
parallel geometry                [Eq. (app-distances)]
  d_LL = d_RR = d_0, d_LR = d_0+Delta,
  d_RL = d_0-Delta
closed form Neg = |sin(phi_ent/2)|/2
                                 [Eq. (app-negativity)]

point U (unscreened): d_0 = 450 um, Delta = 200 um
  d_LL = d_RR = 4.500000e-04 m
  d_LR = 6.500000e-04 m,  d_RL = 2.500000e-04 m
  phi_LL = phi_RR = +1.406326e-01 rad
  phi_LR = +9.736101e-02 rad
  phi_RL = +2.531386e-01 rad
  phi_ent = -6.923450e-02 rad
  Neg (partial transpose) = 1.73051676e-02
  Neg (closed form)       = 1.73051676e-02
  |difference|            = 1.041e-17

point S (screened): d_0 = 35 um, Delta = 1 um
  d_LL = d_RR = 3.500000e-05 m
  d_LR = 3.600000e-05 m,  d_RL = 3.400000e-05 m
  phi_LL = phi_RR = +1.808133e+00 rad
  phi_LR = +1.757907e+00 rad
  phi_RL = +1.861313e+00 rad
  phi_ent = -2.954466e-03 rad
  Neg (partial transpose) = 7.38616184e-04
  Neg (closed form)       = 7.38616184e-04
  |difference|            = 3.307e-17

checks against the numbers the prose prints:
  G m_A m_B / hbar  [App. A]
    got 6.3285e-05  prose 6.33e-05 m s^-1  PASS
  bracket at point U  [App. A]
    got -1094  prose -1090 m^-1  PASS
  |phi_ent| at U  [App. A]
    got 0.069234  prose 0.069 rad  PASS
  Neg_AB at U  [App. A]
    got 0.017305  prose 0.017  PASS
  |phi_ent| at S  [Sec. 4]
    got 0.002954  prose 0.003 rad  PASS
  Neg_AB at S  [Sec. 4]
    got 0.0007386  prose 0.0007  PASS
  sqrt(3)/4 over Neg_AB at S  [Sec. 4]
    got 586.2  prose 600  PASS
  |phi_ent| rate at U  [Sec. 2]
    got 0.069234  prose 0.069 rad s^-1  PASS
  |phi_ent| rate at S  [Sec. 2]
    got 0.002954  prose 0.003 rad s^-1  PASS
  rate ratio U/S  [Sec. 2]
    got 23.43  prose 23  PASS
  t to 1 rad at U  [Sec. 2]
    got 14.44  prose 14 s  PASS
  t to pi at U  [Sec. 2]
    got 45.38  prose 45 s  PASS
  t to 1 rad at S  [Sec. 2]
    got 338.5  prose 340 s  PASS
  t to pi at S  [Sec. 2]
    got 1063  prose 1100 s  PASS
  1/[1-(Delta/d)^2] at U  [Sec. 2]
    got 1.2462  prose 1.2462  PASS

deterministic sweep, phi_ent on 0..2pi, 33 nodes:
  max |numeric - closed form| = 3.331e-16
seeded sweep, 20000 random phase quadruples
  phi_ij ~ U(-pi, pi), default_rng(20260919)
  max |numeric - closed form| = 6.661e-16
  worst case over blocks (a) = 6.661e-16
  closed form reproduced to 1e-12          PASS
========================================================
(b) THE SAME STATE IN THREE PERSPECTIVES
--------------------------------------------------------
axes ordered (A, B, C); the frame body carries the
trivial one-dimensional factor  [Sec. 4 convention]
lab:  |a_i>_A |b_j>_B, C trivial   [Eq. (app-state)]
A:    |a_i>_A|b_j>_B -> |-a_i>_C |b_j-a_i>_B
                                  [Eq. (app-astate)]
B:    |a_i>_A|b_j>_B -> |a_i-b_j>_A |-b_j>_C
orthogonal branch kets: one basis vector per
distinct relative position          [App. A, A.5]

equal arms [Tab. app-frame-negativities]
  Delta_A = 200 um, Delta_B = 200 um, d_0 = 450 um
  phi_ent = -6.923450e-02 rad
  alphabet sizes (dim A, dim B, dim C):
    lab body C  (2, 2, 1)
    mass A      (1, 3, 2)
    mass B      (3, 1, 2)
  computed
  perspective   Neg_A:B    Neg_B:C    Neg_A:C
  lab body C   0.017305   0.000000   0.000000
  mass A       0.000000   0.433013   0.000000
  mass B       0.000000   0.000000   0.433013
  expected
  perspective   Neg_A:B    Neg_B:C    Neg_A:C
  lab body C   0.017305   0.000000   0.000000
  mass A       0.000000   0.433013   0.000000
  mass B       0.000000   0.000000   0.433013
  entry-by-entry, tolerance 1e-6
  perspective    A:B        B:C        A:C
  lab body C   PASS       PASS       PASS
  mass A       PASS       PASS       PASS
  mass B       PASS       PASS       PASS
  9 pass, 0 fail

generic arms [Tab. three-frames caption]
  Delta_A = 200 um, Delta_B = 140 um, d_0 = 450 um
  phi_ent = -4.556787e-02 rad
  alphabet sizes (dim A, dim B, dim C):
    lab body C  (2, 2, 1)
    mass A      (1, 4, 2)
    mass B      (4, 1, 2)
  computed
```

```
  perspective   Neg_A:B    Neg_B:C    Neg_A:C
  lab body C   0.011391   0.000000   0.000000
  mass A       0.000000   0.500000   0.000000
  mass B       0.000000   0.000000   0.500000
  expected
  perspective   Neg_A:B    Neg_B:C    Neg_A:C
  lab body C   0.011391   0.000000   0.000000
  mass A       0.000000   0.500000   0.000000
  mass B       0.000000   0.000000   0.500000
  entry-by-entry, tolerance 1e-6
  perspective   A:B        B:C        A:C
  lab body C   PASS       PASS       PASS
  mass A       PASS       PASS       PASS
  mass B       PASS       PASS       PASS
  9 pass, 0 fail

Lemma (blind): Neg_B:C in A's frame does not move
when every phi_ij is changed.  Recomputed at
phi_ij = 0 (gravity off, G -> 0):
  Neg_B:C (A's frame, gravity off) = 0.433013
  Neg_A:B (lab frame, gravity off) = 0.000000
  equals sqrt(3)/4 = 0.433013               PASS
total table entries: 18 pass, 0 fail
=========================================================
(c) WITNESS FLOW AND DETECTION THRESHOLD
---------------------------------------------------------
C = |sin(phi_ent/2)|, lambda = exp(-gamma t)
W_fix = lambda (1+lambda) sin^2(phi_ent/2)
                                      [Eq. (witfix)]
W_opt = s_1 + s_2 of T(lambda,lambda), that is
  2 lambda C           if C >= lambda
  lambda C + lambda^2  otherwise      [Eq. (witmax)]
separable bound: W <= 1 for every product state

W_opt against s_1+s_2 of T, 85 (phi_ent, gamma t) pairs
  max |s_1+s_2 - W_opt| = 2.220e-16
  singular-value form reproduced           PASS

W_opt(phi_ent) for the dephasing family:
phi_ent   gt=0.00 gt=0.25 gt=0.50 gt=1.00 gt=2.00
0.0000     1.0000  0.6065  0.3679  0.1353  0.0183
0.3927     1.1951  0.7585  0.4862  0.2071  0.0528
0.7854     1.3827  0.9046  0.6000  0.2816  0.1036
1.1781     1.5556  1.0392  0.7048  0.4088  0.1504
1.5708     1.7071  1.1572  0.8578  0.5203  0.1914
1.9635     1.8315  1.2951  1.0086  0.6118  0.2251
2.3562     1.9239  1.4390  1.1207  0.6798  0.2501
2.7489     1.9808  1.5277  1.1898  0.7216  0.2655
3.1416     2.0000  1.5576  1.2131  0.7358  0.2707

W_fix(phi_ent) for the dephasing family:
phi_ent   gt=0.00 gt=0.25 gt=0.50 gt=1.00 gt=2.00
0.0000     0.0000  0.0000  0.0000  0.0000  0.0000
0.3927     0.0761  0.0527  0.0371  0.0192  0.0058
0.7854     0.2929  0.2029  0.1427  0.0737  0.0225
1.1781     0.6173  0.4276  0.3008  0.1553  0.0474
1.5708     1.0000  0.6927  0.4872  0.2516  0.0768
1.9635     1.3827  0.9577  0.6737  0.3479  0.1062
2.3562     1.7071  1.1825  0.8317  0.4295  0.1311
2.7489     1.9239  1.3326  0.9373  0.4841  0.1478
3.1416     2.0000  1.3853  0.9744  0.5032  0.1537

dephasing ceilings, from W <= 1 at C = 1:
  W_fix ceiling, ln[(1+sqrt5)/2]  [App. B]
    got 0.48121  prose 0.481 gamma t  PASS
  W_opt ceiling, ln 2  [App. B]
    got 0.69315  prose 0.693 gamma t  PASS

W_min(N,z) = (N + z sqrt(3N+4z^2))/(N+z^2)
                                        [Eq. (wmin)]
phi_min = 2 arcsin min{W_min e^gt - e^-gt,
                       (1/2) W_min e^gt}
                                      [Eq. (phimin)]
  W_min(1e3, 3.09) = 1.15925
  W_min(1e6, 3.09) = 1.00534

  "--" marks a branch with no real solution: the
  witness cannot reach W_min at that gamma t
phi_ent^min at N = 1e+03, z = 3.09 (rad):
  gamma t   tilted    plain     used
  0.000     0.3199    1.2365    0.3199
  0.250     1.5782    1.6788    1.5782
  0.273     1.7329    1.7315    1.7315
  0.300     1.9369    1.7971    1.7971
  0.500     --        2.5437    2.5437
  0.545     --        3.0870    3.0870
phi_ent^min at N = 1e+06, z = 3.09 (rad):
  gamma t   tilted    plain     used
  0.000     0.0107    1.0534    0.0107
  0.250     1.0752    1.4032    1.0752
  0.500     --        1.9538    1.9538
  0.600     --        2.3156    2.3156
  0.688     --        --        --

checks against the numbers Appendix B prints:
  W_min(1e3, 3.09)
    got 1.1593  prose 1.159  PASS
  phi_min, gt=0, N=1e3, tilted
    got 0.3199  prose 0.32 rad  PASS
  phi_min, gt=0, N=1e3, plain
    got 1.237  prose 1.24 rad  PASS
  ratio plain/tilted at gt=0
    got 3.866  prose 3.9  PASS
  phi_min, gt=0.3, N=1e3
    got 1.797  prose 1.8 rad  PASS
  crossover gamma t
    got 0.27269  prose 0.273  PASS
  ceiling at N=1e3, ln(2/W_min)
    got 0.54537  prose 0.545 gamma t  PASS
  ceiling at N=1e6, ln(2/W_min)
    got 0.68782  prose 0.688 gamma t  PASS
  small-phase prefactor, 2 sqrt 3
    got 3.4641  prose 3.4641  PASS

dephased witness at the scan's own gamma = 1e-3 Hz
  [Sec. 2]; lambda = exp(-gamma t), phi_ent = rate * t
  maximised over t in the plain family W = 2 lambda C,
  which is the setting optimum wherever C >= lambda
  point U: max W = 1.9121 at t = 44.5 s
    lambda = 0.9564, C = 0.9996, C >= lambda: yes
  point S: max W = 0.8556 at t = 660.5 s
    lambda = 0.5166, C = 0.8281, C >= lambda: yes
  point U at t = 45.4 s (phi_ent = pi): W = 1.9113
  screened max witness  [Sec. 2]
    got 0.8556  prose 0.86  PASS
  unscreened witness at pi  [Sec. 2]
    got 1.911  prose 1.91  PASS
=========================================================
FIGURE DATA WRITTEN TO JSON
  fig:three-frames  bars, 3 frames x 3 bipartitions
  fig:witness-flow  W_opt on 5 gamma t curves
=========================================================
SUMMARY
  block (a):  16 pass,   0 fail
  block (b):  19 pass,   0 fail
  block (c):  14 pass,   0 fail
  total:      49 pass,   0 fail
  max |closed form - partial transpose| = 6.661e-16
  three-frame table: 18 pass, 0 fail
=========================================================
```

C.2 The three-frame table

Block (b) reconstructs Table 2 entry by entry and compares each of the nine numbers against the value that table prints, at tolerance 10^{-6}. All nine pass. The laboratory row returns $\mathcal{N}_{AB} = 0.017305$ at point U's $\varphi_{\text{ent}} = -6.923450 \times 10^{-2}$ rad, which is $\frac{1}{2}|\sin(\varphi_{\text{ent}}/2)|$ to fifteen figures, with $\mathcal{N}_{BC} = \mathcal{N}_{AC} = 0$ exactly; mass A's row returns $\mathcal{N}_{BC} = 0.433013 = \sqrt{3}/4$ with the other two exactly zero, and mass B's row the mirror. The dimension triples the script prints alongside them are $(2, 2, 1)$, $(1, 3, 2)$ and $(3, 1, 2)$: two branch registers and a trivial frame in the laboratory description, and in each mass's description a trivial frame, a two-level spectator and the three-level alphabet the coincidence $d_{LL} = d_{RR}$ of Eq. (16) leaves behind.

Nine further entries check the generic-arm variant that Table 1's caption records. With $\Delta_A = 200\,\mu$m against $\Delta_B = 140\,\mu$m the four relative positions $b_j - a_i$ become distinct, the alphabets grow to $(1, 4, 2)$ and $(4, 1, 2)$, and the off-diagonal entries move from $\sqrt{3}/4$ to exactly $1/2$ while the laboratory entry follows its own geometry down to 0.011391. Those nine pass as well, so the table check stands at eighteen passes and no failures. One further evaluation isolates Lemma 2: setting every φ_{ij} to zero, which is the model's $G \to 0$ limit, leaves $\mathcal{N}_{BC}^{(A)} = 0.433013$ unmoved while the laboratory negativity collapses to zero. The frame-changed number is blind to gravity in the strong sense the lemma states, and the script reaches that conclusion by recomputation rather than by reading the proof.

C.3 The witness and threshold checks

Block (c) first verifies the route Appendix B takes to Eq. (26) rather than the formula alone: on eighty-five $(\varphi_{\text{ent}}, \gamma t)$ pairs it builds the dephased correlation matrix of Eq. (27), takes its singular values numerically, and finds $s_1 + s_2$ equal to the two-branch expression $2\lambda C$ or $\lambda C + \lambda^2$ to 2.2×10^{-16}. The dephasing ceilings follow exactly: $\gamma t = 0.48121$ for the fixed-setting form and $\gamma t = 0.69315 = \ln 2$ for the setting-optimal one, against the 0.481 and 0.693 Appendix B quotes.

The threshold arithmetic reproduces every number that appendix prints. $W_{\min}(10^3, 3.09) = 1.15925$ against the quoted 1.159; at $\gamma t = 0$ and $N = 10^3$ the tilted-setting branch of Eq. (30) gives $\varphi_{\text{ent}}^{\min} = 0.3199$ rad and the plain branch 1.2365 rad, a ratio of 3.87 against the quoted factor of 3.9; the crossover sits at $\gamma t = 0.27269$ against the quoted 0.273; and the ceilings $\ln(2/W_{\min})$ are 0.54537 at $N = 10^3$ and 0.68782 at $N = 10^6$, against 0.545 and 0.688. The small-phase limit of the tilted branch returns the prefactor $3.46410 = 2\sqrt{3}$ at $N = 10^{12}$. One line of that appendix is looser than the rest and the printout shows why: at $\gamma t = 0.3$ and $N = 10^3$ the two branches are 1.9369 and 1.7971 rad rather than equal, and what coincides there is the threshold actually used, 1.797 rad, with the quoted 1.80; the branches cross a little earlier, at $\gamma t = 0.27269$, where both give 1.73 rad. The sentence is right about the crossover and right about the number; "coincide" describes the numerical proximity at $\gamma t = 0.3$ and not an equality.

Two evaluations close the loop with §2's comparison of the screened and unscreened geometries at the scan's own 10^{-3} Hz. Maximized over the hold time in the plain setting family, $W = 2\lambda|\sin(\varphi_{\text{ent}}/2)|$, the screened point peaks at 0.8556 at $t = 660.5$ s and the unscreened point at 1.9121 at $t = 44.5$ s, reading 1.9113 at the $t = 45.4$ s where φ_{ent} reaches π; those are the 0.86 and the 1.91 at $t \simeq 45$ s that section quotes. The maximizer satisfies $C \geq \lambda$ in both cases, so the plain family is the setting optimum there and the two readings agree; below that line the optimum is the $\lambda C + \lambda^2$ branch, which tends to unity as $\varphi_{\text{ent}} \to 0$ because a product state saturates the separable bound, and which is therefore not a witness value an experiment achieves. Forty-nine checks run in total across the three blocks and all forty-nine pass; the largest disagreement anywhere between the closed-form negativity and the numerical partial transpose is 6.7×10^{-16}, which is double-precision arithmetic and not a residual.

References

[1] Y. Aharonov, T. Kaufherr (1984). Quantum frames of reference. *Physical Review D, vol. 30, p. 368*. https://doi.org/10.1103/PhysRevD.30.368. DOI: 10.1103/PhysRevD.30.368.

[2] Y. Aharonov, L. Susskind (1967). Charge Superselection Rule. *Physical Review, vol. 155, p. 1428*. https://doi.org/10.1103/PhysRev.155.1428. DOI: 10.1103/PhysRev.155.1428.

[3] P. M. Alsing, I. Fuentes (2012). Observer dependent entanglement. *Classical and Quantum Gravity, vol. 29, article 224001*. https://arxiv.org/abs/1210.2223. DOI: 10.1088/0264-9381/29/22/224001.

[4] P. M. Alsing, G. J. Milburn (2003). Teleportation with a uniformly accelerated partner. *Physical Review Letters, vol. 91, article 180404*. https://arxiv.org/abs/quant-ph/0302179. DOI: 10.1103/PhysRevLett.91.180404.

[5] C. Anastopoulos, B.-L. Hu (2018). Comment on "A Spin Entanglement Witness for Quantum Gravity" and on "Gravitationally Induced Entanglement between Two Massive Particles is Sufficient Evidence of Quantum Effects in Gravity". *arXiv:1804.11315*. https://arxiv.org/abs/1804.11315.

[6] R. M. Angelo, A. D. Ribeiro (2012). Kinematics and dynamics in noninertial quantum frames

of reference. *Journal of Physics A: Mathematical and Theoretical, vol. 45, article 465306*. https://arxiv.org/abs/1204.5627. DOI: 10.1088/1751-8113/45/46/465306.

[7] L. Apadula, E. Castro-Ruiz, Č. Brukner (2024). Quantum Reference Frames for Lorentz Symmetry. *Quantum, vol. 8, article 1440*. https://arxiv.org/abs/2212.14081. DOI: 10.22331/q-2024-08-14-1440.

[8] A. Ballesteros, F. Giacomini, G. Gubitosi (2021). The group structure of dynamical transformations between quantum reference frames. *Quantum, vol. 5, article 470*. https://arxiv.org/abs/2012.15769. DOI: 10.22331/q-2021-06-08-470.

[9] S. D. Bartlett, T. Rudolph, R. W. Spekkens (2007). Reference frames, superselection rules, and quantum information. *Reviews of Modern Physics, vol. 79, pp. 555–609*. https://arxiv.org/abs/quant-ph/0610030. DOI: 10.1103/RevModPhys.79.555.

[10] S. D. Bartlett, T. Rudolph, R. W. Spekkens, P. S. Turner (2006). Degradation of a quantum reference frame. *New Journal of Physics, vol. 8, article 58*. https://arxiv.org/abs/quant-ph/0602069. DOI: 10.1088/1367-2630/8/4/058.

[11] A. Belenchia, R. M. Wald, F. Giacomini, E. Castro-Ruiz, Č. Brukner, M. Aspelmeyer (2018). Quantum superposition of massive objects and the quantization of gravity. *Physical Review D, vol. 98, article 126009*. https://arxiv.org/abs/1807.07015. DOI: 10.1103/PhysRevD.98.126009.

[12] A. Belenchia, R. M. Wald, F. Giacomini, E. Castro-Ruiz, Č. Brukner, M. Aspelmeyer (2019). Information content of the gravitational field of a quantum superposition. *International Journal of Modern Physics D*. https://arxiv.org/abs/1905.04496. DOI: 10.1142/S0218271819430016.

[13] S. Bose, A. Mazumdar, G. W. Morley, H. Ulbricht, M. Toroš, M. Paternostro, A. Geraci, P. Barker, M. S. Kim, G. Milburn (2017). A Spin Entanglement Witness for Quantum Gravity. *Physical Review Letters, vol. 119, article 240401*. https://arxiv.org/abs/1707.06050. DOI: 10.1103/PhysRevLett.119.240401.

[14] S. Bose, I. Fuentes, A. A. Geraci, S. M. Khan, S. Qvarfort, M. Rademacher, M. Rashid, M. Toroš, H. Ulbricht, C. C. Wanjura (2025). Massive Quantum Systems as Interfaces of Quantum Mechanics and Gravity. *Reviews of Modern Physics, vol. 97, article 015003*. https://arxiv.org/abs/2311.09218. DOI: 10.1103/RevModPhys.97.015003.

[15] S. Bose, A. Mazumdar, R. Penrose, I. Fuentes, M. Toroš, R. Folman, G. J. Milburn, M. Kim, A. Kent, et al. (2025). A Spin-Based Pathway to Testing the Quantum Nature of Gravity. *arXiv:2509.01586*. https://arxiv.org/abs/2509.01586.

[16] E. Castro-Ruiz, F. Giacomini, A. Belenchia, Č. Brukner (2020). Quantum clocks and the temporal localisability of events in the presence of gravitating quantum systems. *Nature Communications, vol. 11, article 2672*. https://arxiv.org/abs/1908.10165. DOI: 10.1038/s41467-020-16013-1.

[17] C. Cepollaro, F. Giacomini (2024). Quantum generalisation of Einstein's Equivalence Principle can be verified with entangled clocks as quantum reference frames. *Classical and Quantum Gravity, vol. 41, article 185009*. https://arxiv.org/abs/2112.03303. DOI: 10.1088/1361-6382/ad6d26.

[18] H. Chevalier, A. J. Paige, M. S. Kim (2020). Witnessing the Non-Classical Nature of Gravity in the Presence of Unknown Interactions. *Physical Review A, vol. 102, article 022428*. https://arxiv.org/abs/2005.13922. DOI: 10.1103/PhysRevA.102.022428.

[19] M. Christodoulou, A. Di Biagio, M. Aspelmeyer, Č. Brukner, C. Rovelli, R. Howl (2023). Locally Mediated Entanglement in Linearized Quantum Gravity. *Physical Review Letters, vol. 130, article 100202*. https://arxiv.org/abs/2202.03368. DOI: 10.1103/PhysRevLett.130.100202.

[20] M. Christodoulou, C. Rovelli (2019). On the possibility of laboratory evidence for quantum superposition of geometries. *Physics Letters B, vol. 792, pp. 64–68*. https://arxiv.org/abs/1808.05842. DOI: 10.1016/j.physletb.2019.03.015.

[21] B. Corbeel (2026). Every Interferometer Is Secretly a Clock Comparison. *Absolute Digital Publishers, The Quantum–Relativity Papers, No. 1*. https://absolutedigitalpublishers.com/papers/quantum-relativity-01-clock-comparison.pdf.

[22] B. Corbeel (2026). A Reference Frame Becomes Classical by Publishing Its Orientation. *Absolute Digital Publishers, Revolutionary Life 75, Series D, No. 1*. https://absolutedigitalpublishers.com/papers/revolutionary-life-75-d01-reference-frame-orientatio pdf.

[23] M. Czachor (1997). Einstein-Podolsky-Rosen-Bohm experiment with relativistic massive particles. *Physical Review A, vol. 55, pp. 72–77*. https://journals.aps.org/pra/abstract/10.1103/PhysRevA.55.72. DOI: 10.1103/PhysRevA.55.72.

[24] D. L. Danielson, G. Satishchandran, R. M. Wald (2022). Black Holes Decohere Quantum Superpositions. *International Journal of Modern Physics D, vol. 31, no. 14, article 2241003*. https://arxiv.org/abs/2205.06279. DOI: 10.1142/S0218271822410036.

[25] A.-C. de la Hamette, T. D. Galley (2020). Quantum reference frames for general symmetry groups. *Quantum, vol. 4, article 367*. https://arxiv.org/abs/2004.14292. DOI: 10.22331/q-2020-11-30-367.

[26] A.-C. de la Hamette, T. D. Galley, P. A. Höhn, L. Loveridge, M. P. Müller (2021). Perspective-neutral approach to quantum frame covariance for general symmetry groups. *arXiv:2110.13824*. https://arxiv.org/abs/2110.13824. DOI: 10.48550/arXiv.2110.13824.

[27] U. Delić, M. Reisenbauer, K. Dare, D. Grass, V. Vuletić, N. Kiesel, M. Aspelmeyer (2020). Cooling of a levitated nanoparticle to the motional quantum ground state. *Science, vol. 367, pp. 892–895*. https://arxiv.org/abs/1911.04406. DOI: 10.1126/science.aba3993.

[28] A. Di Biagio (2026). Gravity-induced entanglement is not a theory-independent witness of nonclassicality of the gravitational field. *arXiv:2511.02683; accepted for publication in Physical Review D*. https://arxiv.org/abs/2511.02683.

[29] J. Foo, R. B. Mann, M. Zych (2023). Relativity and decoherence of spacetime superpositions. *arXiv:2302.03259*. https://arxiv.org/abs/2302.03259. DOI: 10.48550/arXiv.2302.03259.

[30] V. Fragkos, M. Kopp, I. Pikovski (2022). On inference of quantization from gravitationally induced entanglement. *AVS Quantum Science, vol. 4, article 045601*. https://arxiv.org/abs/2206.00558. DOI: 10.1116/5.0107839.

[31] T. M. Fuchs, D. G. Uitenbroek, J. Plugge, N. van Halteren, J.-P. van Soest, A. Vinante, H. Ulbricht, T. H. Oosterkamp (2024). Measuring Gravity with Milligram Levitated Masses. *arXiv:2303.03545*. https://arxiv.org/abs/2303.03545.

[32] I. Fuentes-Schuller, R. B. Mann (2005). Alice falls into a black hole: Entanglement in non-inertial frames. *Physical Review Letters, vol. 95, article 120404*. https://arxiv.org/abs/quant-ph/0410172. DOI: 10.1103/PhysRevLett.95.120404.

[33] T. D. Galley, F. Giacomini, J. H. Selby (2022). A no-go theorem on the nature of the gravitational field beyond quantum theory. *Quantum, vol. 6, article 779*. https://arxiv.org/abs/2012.01441. DOI: 10.22331/q-2022-08-17-779.

[34] F. Giacomini (2021). Spacetime Quantum Reference Frames and superpositions of proper time. *Quantum, vol. 5, article 508*. https://arxiv.org/abs/2101.11628. DOI: 10.22331/q-2021-07-22-508.

[35] F. Giacomini, Č. Brukner (2022). Einstein's Equivalence Principle for superpositions of gravitational fields and quantum reference frames. *arXiv:2012.13754*. https://arxiv.org/abs/2012.13754. DOI: 10.48550/arXiv.2012.13754.

[36] F. Giacomini, E. Castro-Ruiz, Č. Brukner (2019). Quantum mechanics and the covariance of physical laws in quantum reference frames. *Nature Communications, vol. 10, article 494*. https://arxiv.org/abs/1712.07207. DOI: 10.1038/s41467-018-08155-0.

[37] F. Giacomini, E. Castro-Ruiz, Č. Brukner (2019). Relativistic quantum reference frames: the operational meaning of spin. *Physical Review Letters, vol. 123, article 090404*. https://arxiv.org/abs/1811.08228. DOI: 10.1103/PhysRevLett.123.090404.

[38] R. M. Gingrich, C. Adami (2002). Quantum Entanglement of Moving Bodies. *Physical Review Letters, vol. 89, article 270402*. https://arxiv.org/abs/quant-ph/0205179. DOI: 10.1103/PhysRevLett.89.270402.

[39] M. J. W. Hall, M. Reginatto (2018). On two recent proposals for witnessing nonclassical gravity. *Journal of Physics A: Mathematical and Theoretical, vol. 51, article 085303*. https://arxiv.org/abs/1707.07974. DOI: 10.1088/1751-8121/aaa734.

[40] N. L. Harshman, K. S. Ranade (2011). Observables can be tailored to change the entanglement of any pure state. *Physical Review A, vol. 84, article 012303*. https://journals.aps.org/pra/abstract/10.1103/PhysRevA.84.012303. DOI: 10.1103/PhysRevA.84.012303.

[41] P. A. Höhn, A. R. H. Smith, M. P. E. Lock (2021). The Trinity of Relational Quantum Dynamics. *Physical Review D, vol. 104, article 066001*. https://arxiv.org/abs/1912.00033. DOI: 10.1103/PhysRevD.104.066001.

[42] P. A. Höhn, A. Vanrietvelde (2020). How to switch between relational quantum clocks. *New Journal of Physics, vol. 22, article 123048*. https://arxiv.org/abs/1810.04153. DOI: 10.1088/1367-2630/abd1ac.

[43] V. Kabel, A.-C. de la Hamette, E. Castro-Ruiz, Č. Brukner (2024). Quantum conformal symmetries for spacetimes in superposition. *Quantum, vol. 8, article 1547*. https://arxiv.org/abs/2207.00021. DOI: 10.22331/q-2024-12-04-1547.

[44] T. Krisnanda, G. Y. Tham, M. Paternostro, T. Paterek (2020). Observable Quantum Entanglement due to Gravity. *npj Quantum Information, vol. 6, article 12*. https://arxiv.org/abs/1906.08808. DOI: 10.1038/s41534-020-0243-y.

[45] M. Krumm, P. A. Höhn, M. P. Müller (2021). Quantum reference frame transformations as symmetries and the paradox of the third particle. *Quantum, vol. 5, article 530*. https://arxiv.org/abs/2011.01951. DOI: 10.22331/q-2021-08-26-530.

[46] L. Lami, J. S. Pedernales, M. B. Plenio (2024). Testing the Quantum Nature of Gravity without Entanglement. *Physical Review X, vol. 14, article 021022*. https://arxiv.org/abs/2302.03075. DOI: 10.1103/PhysRevX.14.021022.

[47] C. Marletto, V. Vedral (2017). Gravitationally Induced Entanglement between Two Massive Particles is Sufficient Evidence of Quantum Effects in Gravity. *Physical Review Letters, vol. 119, article 240402*. https://arxiv.org/abs/1707.06036. DOI: 10.1103/PhysRevLett.119.240402.

[48] C. Marletto, V. Vedral (2020). Witnessing nonclassicality beyond quantum theory. *Physical Review D, vol. 102, article 086012*. https://arxiv.org/abs/2003.07974. DOI: 10.1103/PhysRevD.102.086012.

[49] R. J. Marshman, A. Mazumdar, S. Bose (2020). Locality and Entanglement in Table-Top Testing of the Quantum Nature of Linearized Gravity. *Physical Review A, vol. 101, article 052110*. https://arxiv.org/abs/1907.01568. DOI: 10.1103/PhysRevA.101.052110.

[50] E. Martín-Martínez, T. R. Perche (2023). What gravity mediated entanglement can really tell us about quantum gravity. *Physical Review D, vol. 108, article L101702*. https://arxiv.org/abs/2208.09489. DOI: 10.1103/PhysRevD.108.L101702.

[51] D. Miki, N. Matsumoto, A. Matsumura, T. Shichijo, Y. Sugiyama, K. Yamamoto, N. Yamamoto (2023). Generating Quantum Entanglement between Macroscopic Objects with Continuous Measurement and Feedback Control. *Physical Review A, vol. 107, article 032410*. https://arxiv.org/abs/2210.13169. DOI: 10.1103/PhysRevA.107.032410.

[52] O. Oreshkov, F. Costa, Č. Brukner (2012). Quantum correlations with no causal order. *Nature Communications, vol. 3, article 1092*. https://arxiv.org/abs/1105.4464. DOI: 10.1038/ncomms2076.

[53] M. C. Palmer, F. Girelli, S. D. Bartlett (2014). Changing quantum reference frames. *Physical Review A, vol. 89, article 052121*. https://arxiv.org/abs/1307.6597. DOI: 10.1103/PhysRevA.89.052121.

[54] J. S. Pedernales, K. Streltsov, M. B. Plenio (2022). Enhancing Gravitational Interaction between Quantum Systems by a Massive Mediator. *Physical Review Letters, vol. 128, article 110401*. https://arxiv.org/abs/2104.14524. DOI: 10.1103/PhysRevLett.128.110401.

[55] A. Peres, P. F. Scudo, D. R. Terno (2002). Quantum entropy and special relativity. *Physical Review Letters, vol. 88, article 230402*. https://arxiv.org/abs/quant-ph/0203033. DOI: 10.1103/PhysRevLett.88.230402.

[56] A. Peres, D. R. Terno (2004). Quantum information and relativity theory. *Reviews of Modern Physics, vol. 76, pp. 93–123*. https://arxiv.org/abs/quant-ph/0212023. DOI: 10.1103/RevModPhys.76.93.

[57] H. Pino, J. Prat-Camps, K. Sinha, B. P. Venkatesh, O. Romero-Isart (2018). On-chip quantum interference of a superconducting microsphere. *Quantum Science and Technology, vol. 3, article 025001*. https://arxiv.org/abs/1603.01553. DOI: 10.1088/2058-9565/aa9d15.

[58] S. Rijavec, M. Carlesso, A. Bassi, V. Vedral, C. Marletto (2021). Decoherence Effects in Non-Classicality Tests of Gravity. *New Journal of Physics, vol. 23, article 043040*. https://arxiv.org/abs/2012.06230. DOI: 10.1088/1367-2630/abf3eb.

[59] M. Rossi, A. Militaru, N. Carlon Zambon, A. Riera-Campeny, O. Romero-Isart, M. Frimmer, L. Novotny (2024). Quantum Delocalization of a Levitated Nanoparticle. *arXiv:2408.01264*. https://arxiv.org/abs/2408.01264.

[60] C. Rovelli (1996). Relational Quantum Mechanics. *International Journal of Theoretical Physics, vol. 35, pp. 1637–1678*. https://arxiv.org/abs/quant-ph/9609002.

[61] P. R. Saulson (1984). Terrestrial gravitational noise on a gravitational wave antenna. *Physical Review D, vol. 30, p. 732*. https://journals.aps.org/prd/abstract/10.1103/PhysRevD.30.732. DOI: 10.1103/PhysRevD.30.732.

[62] M. Schut, A. Mazumdar (2025). Parameter Scanning in a Quantum-Gravity-Induced Entanglement of Masses (QGEM) Experiment with Electromagnetic Screening. *arXiv:2502.12474*. https://arxiv.org/abs/2502.12474.

[63] A. R. H. Smith, M. Ahmadi (2019). Quantizing time: Interacting clocks and systems. *Quantum, vol. 3, article 160*. https://arxiv.org/abs/1712.00081. DOI: 10.22331/q-2019-07-08-160.

[64] W. Struyve (2025). Absence of gravitationally induced entanglement in certain semi-classical theories of gravity. *arXiv:2510.20991*. https://arxiv.org/abs/2510.20991.

[65] H. Terashima, M. Ueda (2003). Einstein-Podolsky-Rosen correlation seen from moving observers. *Quantum Information and Computation, vol. 3, pp. 224–228*. https://arxiv.org/abs/quant-ph/0204138.

[66] J. Tilly, R. J. Marshman, A. Mazumdar, S. Bose (2021). Qudits for Witnessing Quantum Gravity Induced Entanglement of Masses Under Decoherence. *Physical Review A, vol. 104, article 052416*. https://arxiv.org/abs/2101.08086. DOI: 10.1103/PhysRevA.104.052416.

[67] D. Trillo, M. Navascués (2025). The Diósi-Penrose model of classical gravity predicts gravitationally induced entanglement. *Physical Review D, vol. 111, article L121101*. https://arxiv.org/abs/2411.02287. DOI: 10.1103/PhysRevD.111.L121101.

[68] T. W. van de Kamp, R. J. Marshman, S. Bose, A. Mazumdar (2020). Quantum Gravity Witness via Entanglement of Masses: Casimir Screening. *Physical Review A, vol. 102, article 062807*. https://arxiv.org/abs/2006.06931. DOI: 10.1103/PhysRevA.102.062807.

[69] A. Vanrietvelde, P. A. Höhn, F. Giacomini, E. Castro-Ruiz (2020). A change of perspective: switching quantum reference frames via a perspective-neutral framework. *Quantum, vol. 4, article 225*. https://arxiv.org/abs/1809.00556. DOI: 10.22331/q-2020-01-27-225.

[70] T. Weiss, M. Roda-Llordes, E. Torrontegui, M. Aspelmeyer, O. Romero-Isart (2021). Large Quantum Delocalization of a Levitated Nanoparticle Using Optimal Control: Applications for Force Sensing and Entangling via Weak Forces. *Physical Review Letters, vol. 127, article 023601*. https://arxiv.org/abs/2012.12260. DOI: 10.1103/PhysRevLett.127.023601.

[71] T. Westphal, H. Hepach, J. Pfaff, M. Aspelmeyer (2021). Measurement of Gravitational Coupling between Millimetre-Sized Masses. *Nature, vol. 591, pp. 225–228*. https://arxiv.org/abs/2009.09546. DOI: 10.1038/s41586-021-03250-7.

[72] P. Zanardi (2001). Virtual Quantum Subsystems. *Physical Review Letters, vol. 87, article 077901*. https://arxiv.org/abs/quant-ph/0103030. DOI: 10.1103/PhysRevLett.87.077901.

[73] P. Zanardi, D. A. Lidar, S. Lloyd (2004). Quantum Tensor Product Structures Are Observable Induced. *Physical Review Letters, vol. 92, article 060402*. https://arxiv.org/abs/quant-ph/0308043. DOI: 10.1103/PhysRevLett.92.060402.

[74] W. H. Zurek (2003). Decoherence, einselection, and the quantum origins of the classical. *Reviews of Modern Physics, vol. 75, pp. 715–775*. https://arxiv.org/abs/quant-ph/0105127. DOI: 10.1103/RevModPhys.75.715.

[75] M. Zych, F. Costa, I. Pikovski, Č. Brukner (2019). Bell's theorem for temporal order. *Nature Communications, vol. 10, article 3772*. https://arxiv.org/abs/1708.00248. DOI: 10.1038/s41467-019-11579-x.